NTNU
Det skapende universitet

TKP4580 1 Kjemisk prosessteknologi, fordypningsprosjekt

Kandidat 10003

Oppgaver	Oppgavetype	Vurdering	Status
1 Handing in the specialization report.	Filopplasting	Manuell poengsum	Levert

TKP4580 1 Kjemisk prosessteknologi, fordypningsprosjekt

Emnekode	TKP4580	PDF opprettet	19.12.2016 10:15
Vurderingsform	TKP4580	Opprettet av	Hege Johannessen
Starttidspunkt:	30.11.2016 10:00	Antall sider	71
Sluttidspunkt:	16.12.2016 15:45	Oppgaver inkludert	Ja
Sensurfrist	Ikke satt	Skriv ut automatisk rettede	Ja

Seksjon 1

1 OPPGAVE

Handing in the specialization report.

Here you can upload your project report.
Only .pdf files are accepted.

Mark the file name with name_research group_supervisor!

Click here to upload your file

BESVARELSE

Filopplasting

Filnavn	10163874_cand-12020524_9125253
Filtype	pdf
Filstørrelse	2714.47 KB
Opplastingstid	15.12.2016 22:53:54

Neste side
Besvarelse vedlagt

NTNU
Norges teknisk-naturvitenskapelige universitet
Fakultet for naturvitenskap og teknologi
Institutt for kjemisk prosessteknologi

SPECIALIZATION PROJECT 2016

TKP4580

PROJECT TITLE:

Modeling and Simulation of Subsea Pipe Separators for Oil and Gas Applications

By

Melissa Florine Dlima

Supervisor for the project:
Prof. Sigurd Skogestad

Date: 16/12/2016

Norwegian University of Science and Technology

NTNU

Department of Chemical Engineering

Modeling and Simulation of a Pipe Separator for Subsea Oil and Gas Applications

Specialization Project

by

Melissa Florine Dlima

Supervisor: Prof. Sigurd Skogestad

Co-Supervisor: Dr. Christoph J. Backi

December 15, 2016

Abstract

This work focuses on modeling and simulation of three phase compact subsea pipe separators for oil and gas applications. Pipe separators use the same principles as that of gravity separators, i.e, the density difference between the phases and the gravitational forces to attain separation. Although the phenomena like coalescence and the droplet breakage are common, for the purpose of simplicity, it is assumed that these phenomena do not occur. The main modeling principle used to describe the oil droplets rising from the water phase to the interface and the water droplets settling from the oil phase into the interface is given by Stokes' law, which gives the rising and settling velocities of the droplets in the phases. It is assumed that the gas enters the separator and immediately flashes out, and hence no liquid droplets are assumed in the gas phase and vice versa.

Nonlinear dynamic equations were derived for the water level, total liquid level and for the pressure of the gas in the system based on the inflow and outflow dynamics and were implemented in MATLAB Simulink using subsystem blocks for each model. The equations were nonlinear due to the geometry of the separator. A static droplet size distribution was assumed for a set of droplet size classes. Based on the horizontal and the vertical residence times of the droplets in the separator, the volume of dispersed water leaving the oil phase and the volume of dispersed oil leaving the water phase were evaluated. Consequently, the separation efficiency was evaluated both for the removal of oil from the water phase and for the water from the oil phase.

Three PI controllers were employed to control the level of water, total liquid level and gas pressure in the system. The PI controllers were tuned and tuning parameters were obtained using open loop step response method and the SIMC tuning rules.

Simulations were carried out for the gravity separator to compare the separation efficiency for different initial separation values at the beginning and towards the end of the reservoir lifetime. The simulation parameters were taken from [1,2]. Additionally, the separation efficiency of the horizontal pipe separators was analysed in comparison to the gravity separators. The performance of a pipe separator for various diameters was studied. In addition to this, the efficiency of separation was analysed for two different cases of parallel pipe separator arrangements.

Preface

This specialization project report was written for the process systems engineering group at the Norwegian University of Science and Technology. The work was carried out during the Fall of 2016 at the Department of Chemical Engineering.

I would like to thank my supervisor Prof. Sigurd Skogestad for guidance and useful discussions during my work. I would also like to thank my co-supervisor Dr. Christoph Backi for support throughout the project, for providing the technical background on which this project is based and for reviewing the project report. I am grateful for the opportunities given by the process systems engineering group to participate in the meetings and discussions.

Declaration of Compliance

I declare that this is an independent work according to the exam regulations of the Norwegian University of Science and Technology (NTNU).

Trondheim, Norway

December 16, 2016

Melissa Florine Dlima

Contents

List of Figures

List of Tables

List of symbols

Latin Letters

Symbols	Description	Unit
A_L	Cross sectional area of liquid in the separator	m^2
A_O	Cross sectional area of water in the separator	m^2
A_p	Reference area of the droplet	m^2
A_W	Area of water in the separator	m^2
C_d	Drag Coefficient	-
d	Disturbance vector	-
F_b	Buoyant force	N
F_d	Drag force	N
F_g	Gravitational force	N
g	Acceleration due to gravity	ms^{-2}
h_L	Liquid level	m
$h_{L,sp}$	Liquid level setpoint	m
h_O	Oil level	m
h_W	Water level	m
$h_{W,sp}$	Water level setpoint	m
I	Integral term in PID controller	-
K_c	Controller gain for series form	-
$K_c^{'}$	Controller gain for parallel form	-
k	Plant gain	-
N_{Re}	Reynolds number	-
n	Initial number of droplets	-
n_G	Amount of gas	$moles$
P	Proportional term in PID controller	-
p	System pressure	bar
p_{sp}	System pressure set point	bar
$q_{G,in}$	Gas inflow	m^3s^{-1}
$q_{G,out}$	Gas outflow	m^3s^{-1}
$q_{L,in}$	Liquid inflow	m^3s^{-1}
$q_{L,out}$	Liquid outflow	m^3s^{-1}
$q_{W,in}$	Water inflow	m^3s^{-1}
$q_{W,out}$	Water outflow	m^3s^{-1}

Symbols	Description	Unit
R	Universal gas constant	$Jmol^{-1}K^{-1}$
r	Radius	m
T	Temperature	K
u	Vector of manipulated variables	-
V_G	Volume of gas in the separator	m^3
V_L	Volume of liquid in the separator	m^3
V_{Sep}	Volume of the separator	m^3
v_h	Horizontal velocity	ms^{-1}
v_v	Vertical velocity	ms^{-1}
x	Vector of state variables	-

Greek Letters

Symbols	Description	Unit
α	Water cut	-
β	Oil cut	-
η_O	Efficiency of oil	-
η_W	Efficiency of water	-
μ_O	Viscosity of oil	$kg(ms)^{-1}$
μ_W	Viscosity of water	$kg(ms)^{-1}$
ϕ_{oo}	Fraction of oil entering the oil phase	-
ϕ_{ow}	Fraction of oil entering the water ohase	-
ϕ_{wo}	Fraction of water entering the oil phase	-
ϕ_{ww}	Fraction of water entering the water phase	-
ρ_G	Density of gas	kgm^{-3}
ρ_O	Density of oil	kgm^{-3}
ρ_W	Density of water	kgm^{-3}

1 Introduction

The recent interest in subsea processing is mainly motivated by the advantages of reduced pumping cost, water management cost and reduced environmental impact due to water re-injection [3]. Also subsea processing makes it possible to use smaller or no platforms at all, due to the fact that processing equipment is used on the seabed rather than topside [4].

An important aspect of subsea processing is the development of compact subsea technologies. Compact separators are smaller in size compared to the conventional separators, and thus they can reduce the expenditure for developments in deepwater. The parameters of the reservoir, changes through its production cycle and the conventional large separation vessels lack the flexibility with respect to the modification of equipment capacity and size. In deepwater applications, the conventional gravity separators have a major disadvantage owing to its large diameter, size and weight. Installation of these huge vessels on the seabed at greater depths is difficult. Hence, the concept of compact subsea separation is considered to be a key aspect of subsea processing [3].

In recent years the deep water discoveries have accelerated the development of compact separation technologies. The first subsea separator system installed in the world is Troll Pilot followed by Tordis system which was enabled for higher flow rates. Owing to the limitation of conventional huge gravity separators in Troll and Tordis, a compact subsea pipe separator was installed in the Marlim field. This pipe separator works on the same principle as that of the gravity separators [4].

Other than these installed subsea separators, several compact separators are being developed. Saipem is currently developing a system called SpoolSep, a liquid separation system based on the idea of gravity separation to overcome the limitation of large sized gravity separators. Here, the entering fluid is distributed into several pipes which are placed parallel to each other. The SpoolSep can have flexible operation and the parallel pipes can be fitted or removed independently [5]. StatoilHydro and FMC Technologies studied a subsea pipe separator for the use of low pressure production which was tied to the Troll B Floating Production Unit (FPU). The separator was developed by Hydro and was investigated for the liquid-liquid separation in order to remove bulk water from the oil [6].

Recently DEMO2000, a project supported by the Norwegian Ministry of Petroleum and Energy was executed from 2009 to 2011 aiming at compact gas liquid separation systems for deepwater applications [7]. The work focused on compact MultiPipe slug catchers which could possibly provide subsea gas liquid separation. The main idea of the MultiPipe slug catcher is to distribute the multiphase flow into several pipes in order to dampen the flow disturbances and to provide short residence time for the droplets or bubbles. This MultiPipe slug catcher has an inlet followed by a distribution header and the flow is divided into each parallel pipe separators. The separation principle is the same as the conventional

gravity separator. Several tests were conducted over wide ranges of operating conditions. The results reveal a significant drop in separation performance and a high liquid carry over at a velocity above critical superficial gas velocity [7]. Seabed Separation is a company currently doing its research on a dual pipe separator. Here, many small pipes are used rather than a single large separator vessel. The pipe modules could be installed or taken out depending on the phase of the reservoir production and that the system can be modified for the operational conditions rather than limiting the production [8].

Along with companies actively seeking new compact separation technologies, the research community has also started to focus on developing pipe separators. Until now not much research has been done on the use of pipes as separators. Here, some of the existing work on this subject is summarized. [9] studied the Liquid – Liquid Pipe Separator (LLPS) in an integrated compact multiphase Inline Water separation (IWS) system where the pipe was tested and optimized for maximum separation efficiency. [10] carried out experiments and theoretically investigated the developing region (water cut is non zero in the oil phase and vice versa) in oil water flow in horizontal pipe. He developed hydrodynamic and coalescence models to estimate the flow evolution in the developing region of Horizontal Pipe Separator (HPS). He considered three layers each for the water continuous and the oil continuous flow. The hydrodynamic model used momentum balance between the layers and the coalescence model considered population balance equations to take into account the evolution of droplets. [11] proposed design methodology on the hydrodynamic flow behaviour of oil water mixture in the HPS. He claimed that his model could be used for prediction of water fraction at the outlet of the pipe separator.

However, these studies do not consider a dynamic and control oriented approach . Hence, in this report control related models for pipe separators have been derived. Also, the performance of placing several pipe separators in parallel arrangements is studied.

The rest of the report is organized as follows. Chapter 2 gives background information on the movement of droplets in the fluid, description of horizontal pipe separators and general understanding of process control. Chapter 3 presents the control oriented models. Chapter 4 provides the details of the controllers that were employed and their tuning parameters. Chapter 5 describes the simulation results and finally the last chapter provides conclusion and further work.

2 Background

This chapter presents the concept of particle motion in the fluid, a brief description of the horizontal pipe separator and an overview of process control in general.

2.1 Particle movement through the fluid

To understand the separation process, it is important to understand emulsions. An emulsion is a dispersion of one liquid in another liquid, both liquids immiscible with each other. The phase in which the droplets are present is the continuous phase and the droplets are termed as dispersed phase. The main principle of gravity separation is the separation of droplets based on density differences and gravitational forces. The forces exerted on the droplets are the drag force, buoyant force and the gravitational forces as shown in Figure 2.1.

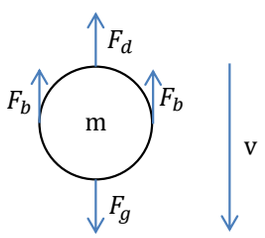

Figure 2.1: Forces acting on a droplet settling through a continuous phase.

The drag force also known as the frictional force will be exerted on the droplet in the viscous fluid. This force is always in the direction opposite to the velocity of the droplet and is given by

$$F_d = \frac{C_D\, v^2\, \rho\, A_p}{2}, \tag{2.1}$$

where C_D is the drag coefficient, v is the relative velocity of the droplet with respect to the surrounding fluid, ρ is the density of the surrounding fluid and A_p is the reference area of the droplet.

The droplet experiences an upward force which opposes the weight of the particle and is termed the buoyant force given by

$$F_b = V_p\, \rho\, g, \tag{2.2}$$

where V_p is the volume of the droplet and g is the acceleration due to gravity.

In addition to the drag and the buoyant force, the particle is exposed to the gravitational force given by

$$F_g = V_p \, \rho_p \, g, \tag{2.3}$$

where ρ_p is the density of the droplet.

The drag coefficient C_D depends on the Reynolds number and it can be defined for several flow regions. For laminar flow, Stokes' law is applied and the drag coefficient is given by

$$C_D = \frac{24}{N_{Re}}, \tag{2.4}$$

where the Reynolds number N_{Re} is given by

$$N_{Re} = \frac{d_p \, v \, \rho}{\mu}, \tag{2.5}$$

where d_p is the diameter of the droplet and μ is the viscosity of the medium in which the droplet is present.

At equilibrium, gravitational force on the particle is equal to the drag force and the buoyant force. Examining equations (2.1), (2.2), (2.3) for the forces acting on the particle, yields the terminal velocity of the particle in the laminar flow, assuming Stokes' law valid and is given by

$$v = g d_p^2 \frac{(\rho_p - \rho)}{18\mu}. \tag{2.6}$$

2.2 Horizontal Pipe Separator Description

This project focuses on three phase pipe separator for the removal of gas from oil and water phase in addition to the separation of oil and water. The pipe separator utilizes one or many small diameter pipes for the separation of oil, gas and water for subsea applications. The concept of pipe separation is based on the principle of density difference between the phases and the gravitational forces as introduced in section 2.1. The three phase mixture enters the separator and separates into the oil, water and the gas phase. The level of water is controlled using the valve at the water outlet, the liquid level comprising of both oil and water is controlled using the oil outlet and the water outlet valve, and the system pressure is controlled using the valve at the gas outlet. Figure 2.2 shows the schematic of three phase pipe separator.

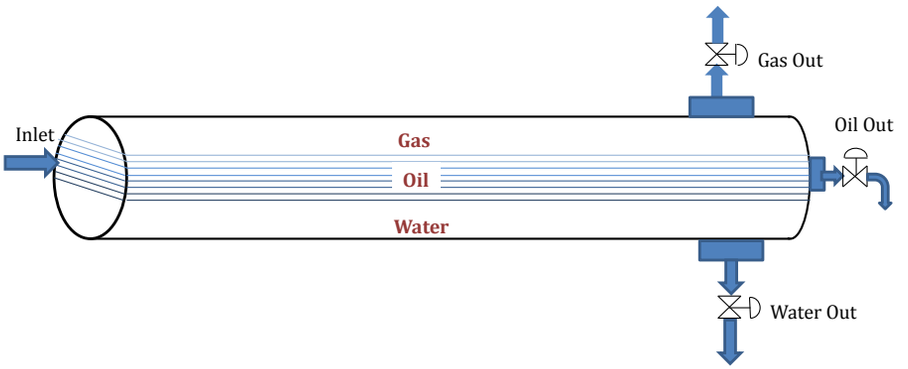

Figure 2.2: Schematic of three phase horizontal pipe separator.

2.3 Process Control

Chemical processes are designed and operated for producing value added products. The processes need to be operated to meet the production objectives including the process safety, environmental regulations, increased profitability. This can be achieved by continuously measuring process variables like level, flow, temperature and by taking actions so that the variables remain at the desired set points. It is necessary to meet the production objectives when the process is subjected to disturbances like the change in the feed flow rate, change in the surrounding temperature etc. and thus necessitates the use of automatic process control. The main objective of process control is to maintain a process at the desired operating conditions in a safe and efficient manner such that the environmental and product quality specifications are satisfied.

The two fundamental control principles under the closed-loop system are the following.

- Feedforward Control: It measures the disturbances and takes corrective action before they disturb the process. However, it requires the disturbance variables to be measured online which is not practical in many applications. It also requires an approximate process model and achieving perfect control in this case may not be realizable.
- Feedback Control: This controller takes action only after the disturbance has upset the system and a non zero error signal is generated. In this case, a good and a fast measurement of the output signal is required.

The desirable characteristics provided by the feedback control system are the following [12].

- Disturbance rejection: The ability of the controller to keep the controlled variable at its desired

set-point in spite of the occurrence of disturbances.

- Set-point tracking: The ability of the controller to move the process variable from one set-point to a new desired set-point.

The general process control system can be viewed as in Fig. 2.3.

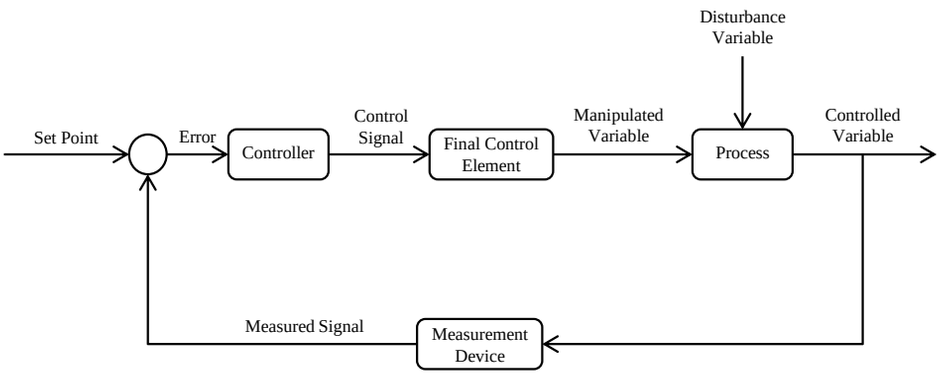

Figure 2.3: Generalized schematic of process control system.

The controller interprets and adjusts for the deviation between the set-point and the measured variable and sends signal to the final control element (e.g control valve) which provides an input to the process to return the controlled variable to the desired set-point.

2.3.1 PID Control

Apart from the on-off control, Proportional Integral Derivative (PID) control is the dominant type of feedback control used in the industry [13]. It is the combination of proportional, integral and the derivative control modes.

The PID control algorithm in its ideal form is given by

$$u(t) = \bar{u} + K_c\Big[e(t) + \frac{1}{\tau_I}\int_0^t e(t)dt + \tau_D\frac{de(t)}{dt}\Big], \tag{2.7}$$

where e(t) is the error between setpoint and measured variable. The constants K_c, τ_I, and τ_D correspond to the controller gain, integral time and the derivative time respectively.

The corresponding transfer function is given by

$$\frac{U(s)}{E(s)} = K_c\Big[1 + \frac{1}{\tau_I s} + \tau_D s\Big]. \tag{2.8}$$

The Proportional part (P-term) is the main part of controller. However, it gives a steady state offset. The addition of integral part (I-term) facilitates the elimination of offset after the change in set point. Although, it is very important to have the offset eliminated, the integral controller is rarely used alone since little control action takes place until the error signal continues to exist. On the other hand, proportional control takes instant corrective action the moment the error is detected. As a result, integral control is usually used together with the proportional control as a PI controller. The derivative control predicts the future behaviour of error signal by considering the change in the derivative of error.

In practice many variations of PID control are being used. The most common forms being the parallel form, the series form and the expanded form of PID control [13].

The *Series (cascade) form of PID controller* is given by

$$c(s) = K_c\Big(\frac{\tau_I s + 1}{\tau_I s}\Big)(\tau_D s + 1), \tag{2.9}$$

where K_c, τ_I and τ_D are the settings for the series form of PID controller.

The *Parallel (ideal) form of PID controller* is given by

$$c'(s) = K_c'\Big(1 + \frac{1}{\tau_I' s} + \tau_D' s\Big), \tag{2.10}$$

where K_c', τ_I' and τ_D' are the settings for the parallel form of PID controller. These can be derived easily by comparing (2.9) with (2.10) and the following translation laws apply:

$$K_c' = K_c\Big(1 + \frac{\tau_D}{\tau_I}\Big); \qquad \tau_I' = \tau_I\Big(1 + \frac{\tau_D}{\tau_I}\Big); \qquad \tau_D' = \frac{\tau_D}{1 + \frac{\tau_D}{\tau_I}}.$$

2.3.2 SIMC - PID Controller Tuning

Although the PID controllers have three parameters, it is difficult to find good settings without using a systematic procedure. Sigurd Skogestad derived the SIMC (Skogestad Internal Model Control) rules [14] for PID controller tuning that are simple and yield good closed-loop behavior. The tuning rules developed by him are model based and can be derived analytically.

Previously, there were quite a few scholars who worked on tuning of PID controllers. The disadvantages of Ziegler - Nichols tuning was that the settings were aggressive, there was no tuning parameter and that the performance was poor for processes with large time delay. The IMC- PID (Lambda tuning) settings by Rivera et al. [15] gave poor disturbance response for integrating process. The SIMC tuning rule works

well for integrating processes, pure time delay processes and for the setpoints and load disturbances. This rule has just one tuning parameter τ_c which is called the desired closed - loop response time.

As stated earlier, the SIMC rule requires a model for tuning. Hence, the first step is to obtain an approximate first or second order time delay model. The first order time delay model is given by

$$g_1(s) = \frac{k}{\tau_1 s + 1} e^{-\theta s}. \tag{2.11}$$

Therefore it is necessary to estimate the model information such as plant gain (k), dominant lag time constant (τ_1) and the dead time (θ). This can be obtained from many ways like the open loop step response, closed loop setpoint response with P-controller or approximation of effective delay using half rule.

In the open loop step response experiment, step change in the manipulated variable (MV) is done one at a time and the output or the controlled variables (CV) are recorded.

For series (cascade) form of PID controller, the SIMC controller settings are given by

$$K_c = \frac{1}{k} \frac{\tau_1}{\tau_c + \theta}, \tag{2.12}$$

$$\tau_I = min\{\tau_1, 4(\tau_c + \theta)\}, \tag{2.13}$$

where k, τ_1 and θ are obtained from Figure 2.4.

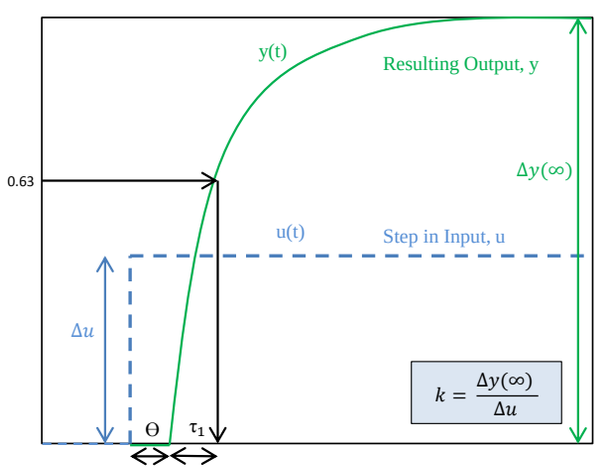

Figure 2.4: Open-loop step response experiment to obtain model parameters for a first order model.

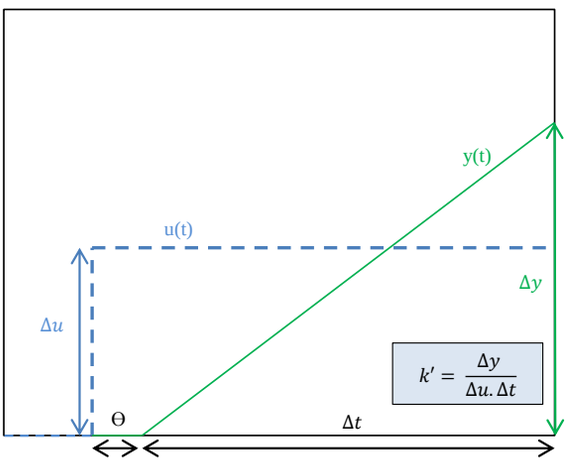

Figure 2.5: Open-loop step response experiment to obtain model parameters for an integrating model.

Since integrating processes have a large time constant, the first order model given by (2.11) can be approximated as

$$g'(s) = \frac{k' e^{-\theta s}}{s}, \tag{2.14}$$

where $k' = \frac{k}{\tau_1}$. The slope of integrating response is k' and is obtained as shown in Figure 2.5.

3 Modeling of the process

This section describes the models for the horizontal pipe separator and the assumptions that are made to simplify the model.

3.1 Assumptions

- Absence of emulsion layer in the separator which means that the droplets will either rise or fall from the interface to disperse in the continuous phases.
- Plug flow model for both the oil and the water phase.
- Absence of coalescence and breakage of the droplets.
- *Stokes' law* is applied for the rising and the settling velocity of the water and oil droplets.
- There are neither water nor oil droplets dispersed in the gas phase and no gas droplets dispersed in the water and oil phases respectively.

3.2 Mathematical Models

This section describes the models for the horizontal pipe separator. The simplified schematic of the pipe separator is illustrated in Figure 3.1. The liquid enters the separator with molar flow rate $q_{L,in}$ and the gas flow rate into the separator is $q_{G,in}$. The incoming liquid is a mixture of water and oil and the volume fraction of water in the liquid is termed water cut α, whereas the volume fraction of oil is termed oil cut $\beta = 1 - \alpha$. As the liquid enters the separator, some of the water droplets disperse into the bulk oil phase which is denoted by ϕ_{wo}. It follows that out of inflowing water, the fraction of water entering the water homogeneous phase is $\phi_{ww} = 1 - \phi_{wo}$. Similarly, some of the oil droplets will disperse into the bulk water phase which is denoted by ϕ_{ow}. Therefore, the fraction of the inflowing oil entering the homogeneous oil phase is $\phi_{oo} = 1 - \phi_{ow}$.

The objective is to control the levels of water, oil and the system pressure and to calculate the amount of dispersed phase in the bulk phase outlets. The variables in the model are classified as state variables $x = [h_L\ h_W\ p]$, manipulated variables $u = [q_{W,out}\ q_{O,out}\ q_{G,out}]$ and the disturbance variable $d = [q_{L,in}]$.

Sections 3.2.1 through 3.2.6 have been implemented in MATLAB/Simulink to calculate the level of liquid and water, horizontal and vertical velocities, residence times in order to reach the interface and the bulk outlet, and to calculate the separation efficiencies in both oil and water phases.

3.2.1 Inventory Models

In this section, non-linear dynamic models are derived representing the change in water level, total liquid level, which includes the oil and the water level, as well as the system pressure. Figure 3.1 illustrates the simplified schematic of the separation process indicating the water level, the total liquid level, the inlet and the outlet sections.

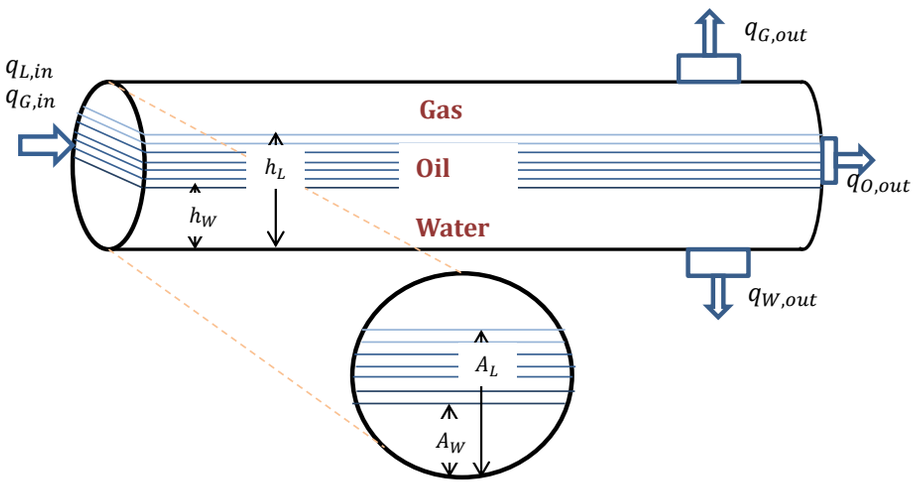

Figure 3.1: Schematic of the three phase horizontal pipe separator indicating heights of inventory.

A. **Rate of change of water level**

The mass balance for the water phase is given by

$$\frac{dm_W}{dt} = \rho_{in} q_{W,in} - \rho_{out} q_{W,out}.$$

Assuming the constant water density, the rate of change of water volume is given as

$$\frac{dV_W}{dt} = q_{W,in} - q_{W,out}. \tag{3.1}$$

The inflowing water contains dispersed oil droplets, and hence $q_{w,in}$ is given by

$$q_{W,in} = q_{L,in}(\alpha\phi_{ww} + \beta\phi_{ow}).$$

Hence, the rate of change of water volume is

$$\frac{dV_W}{dt} = q_{L,in}(\alpha\phi_{ww} + \beta\phi_{ow}) - q_{W,out}.$$

The volume of water contained in the separator is $V_W = A_W L$, where L is the length of the separator, A_W is the cross sectional area of the circular segment containing water with water height h_W as indicated in Figure 3.1.

Therefore the change in area is given by

$$\frac{dA_W}{dt} = \frac{1}{L}\frac{dV_W}{dt}.$$

The cross sectional area of the circular segment filled with water A_W is calculated as

$$A_W = \frac{r^2}{2}\left[2\cos^{-1}\left(\frac{r-h_W}{r}\right) - \sin\left(2\cos^{-1}\left(\frac{r-h_W}{r}\right)\right)\right]. \tag{3.2}$$

In order to obtain the differential equation for the height of water level, the time derivative of (3.2) is given by

$$\frac{dA_W}{dt} = \left[r^2\left(\frac{1-\cos\left(2\cos^{-1}\left(\frac{r-h_W}{r}\right)\right)}{\sqrt{h_W(2r-h_W)}}\right)\right]\frac{dh_W}{dt}. \tag{3.3}$$

Therefore the differential equation for the height of water level is

$$\frac{dh_W}{dt} = \frac{\sqrt{h_W(2r-h_W)}}{r^2L\left(1-\cos\left(2\cos^{-1}\left(\frac{r-h_W}{r}\right)\right)\right)}\frac{dV_W}{dt}. \tag{3.4}$$

B. **Rate of change of total liquid level**

The rate of change of liquid volume in the separator is given by

$$\frac{dV_L}{dt} = q_{L,in} - q_{L,out}. \tag{3.5}$$

The total outflow is the amount of oil and water leaving the separator. Therefore the equation is rewritten as

$$\frac{dV_L}{dt} = q_{L,in} - q_{W,out} - q_{O,out}.$$

The volume of the segment in which the liquid is contained is given by $V_L = A_L L$ where A_L is the cross sectional area of the cylindrical segment containing total liquid.

The above equation can be rewritten as

$$L\frac{dA_L}{dt} = q_{L,in} - q_{W,out} - q_{O,out}.$$

The rate of change of liquid cross sectional area is

$$\frac{dA_L}{dt} = \frac{1}{L}(q_{L,in} - q_{W,out} - q_{O,out}).$$

The cross sectional area of the circular segment containing the total liquid A_L is calculated as

$$A_L = \frac{r^2}{2}\left[2\cos^{-1}\left(\frac{r-h_L}{r}\right) - \sin\left(2\cos^{-1}\left(\frac{r-h_L}{r}\right)\right)\right]. \tag{3.6}$$

In order to obtain the rate of change of liquid level, (3.6) is differentiated with time,

$$\frac{dA_L}{dt} = \left[r^2\left(\frac{1-\cos\left(2\cos^{-1}\left(\frac{r-h_L}{r}\right)\right)}{\sqrt{h_L(2r-h_L)}}\right)\right]\frac{dh_L}{dt}. \tag{3.7}$$

Therefore, the differential equation for height of the liquid is

$$\frac{dh_L}{dt} = \frac{dV_L}{dt}\frac{\sqrt{h_L(2r-h_L)}}{r^2L\left(1-\cos\left(2\cos^{-1}\left(\frac{r-h_L}{r}\right)\right)\right)}. \tag{3.8}$$

C. **Rate of change of system pressure:**

As mentioned previously in the Section 3.1, the gas phase of the separator is modeled by taking the ideal gas law into account. The ideal gas law is given by

$$\bar{p}V_G = n_G RT, \tag{3.9}$$

and $V_G = V_{Sep} - V_L$, where V_{sep} is the total volume of the separator and V_G is the volume of the separator containing the gas phase both measured in cubic metres, $\bar{p}$ is the system pressure measured in pascals, n_G is the number of gas moles, R is the universal gas constant, T is the temperature measured in Kelvin.

The ideal gas law given by (3.9) is differentiated, yielding

$$V_G\frac{d\bar{p}}{dt} + \bar{p}\frac{dV_G}{dt} = RT\frac{dn_G}{dt} + n_G R\frac{dT}{dt}.$$

Assuming isothermal compression, the above equation reduces to

$$V_G\frac{d\bar{p}}{dt} + \bar{p}\frac{dV_G}{dt} = RT\frac{dn_G}{dt}.$$

Since the volume of the gas phase in the separator is inversely proportional to the total liquid phase volume, volume change of the gas phase is given by

$$\frac{dV_G}{dt} = -\frac{dV_L}{dt} = q_{L,in} - q_{W,out} - q_{O,out}. \tag{3.10}$$

The component balance for the gas phase is given by

$$\frac{dn_G}{dt} = -\frac{\rho_G}{M_G}(q_{G,in} - q_{G,out}). \tag{3.11}$$

Using (3.10) and (3.11) the gas pressure dynamics is written as

$$V_G\frac{d\bar{p}}{dt} = RT\frac{\rho_G}{M_G}(q_{G,in} - q_{G,out}) + \bar{p}(q_{L,in} - q_{L,out}), \tag{3.12}$$

and $\bar{p} = p * 10^5$, where p is measured in bars.

The scaled form of (3.12) is thus given by

$$\frac{d(\bar{p} * 10^{-5})}{dt} = \frac{RT}{V_G}\frac{\rho_G}{M_G}(q_{G,in} - q_{G,out}) + (p * 10^5)(q_{L,in} - q_{L,out}). \tag{3.13}$$

3.2.2 Droplet size distribution

As stated in section 3.1, it is assumed that there is absence of coalescence or breakage of the droplets in the separator. Therefore a fixed droplet size distribution is assumed. Droplet sizes of 10 classes were defined as shown in Table 3.1.

Table 3.1: Droplet size distribution.

Droplet size class	Droplet size μm	Number of droplets
1	50	1e8
2	100	5e8
3	150	1e9
4	200	5e9
5	250	1e10
6	300	1e10
7	350	5e9
8	400	1e9
9	450	5e8
10	500	1e8

3.2.3 Horizontal Velocity

As the mixture enters the pipe separator, it is divided into the water continuous phase and the oil continuous phase, each of these phases containing dispersed oil and water droplets respectively. As the continuous phase moves in the horizontal direction towards the outlet, the dispersed droplets move relative to its continuous phase. Therefore the horizontal velocity of the droplets is assumed to be equal to the continuous phase in which they are present.

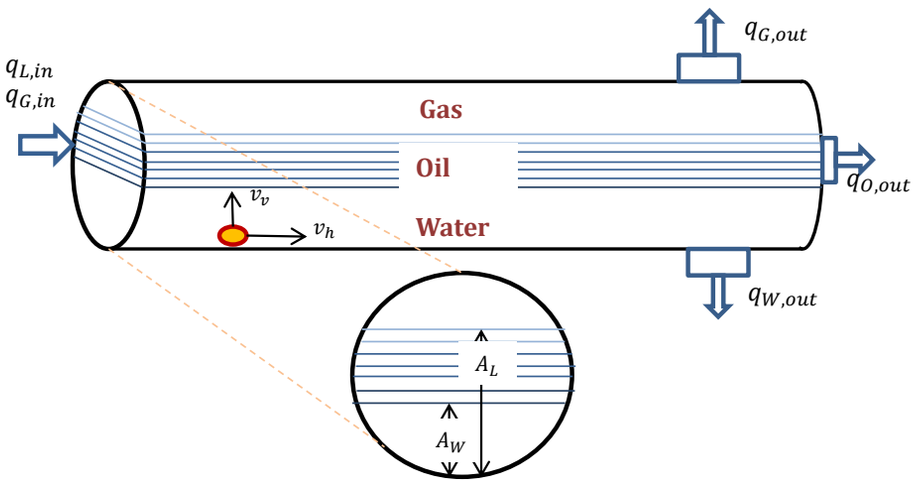

Figure 3.2: Schematic of the three phase pipe separator indicating velocity components on the droplets.

A. **Horizontal velocity of the water droplets**

$$v_h^{water} = \frac{q_{O,in}}{A_O}, \tag{3.14}$$

where $q_{O,in}$ is the flow rate of the oil into the oil continuous phase and A_O is the area of the circular segment containing the oil phase in which the water droplets are being dispersed.

The area of the segment containing oil is obtained using (3.2) and (3.6) and is given by $A_O = A_L - A_W$.

The total flow rate of the oil $q_{O,in}$ is the sum of the oil entering the oil continuous phase and the oil dispersed into the water phase

$$q_{O,in} = q_{L,in}\big(\beta\phi_{oo} + \alpha\phi_{wo}\big)$$

.

B. **Horizontal velocity of the oil droplets**

$$v_h^{oil} = \frac{q_{W,in}}{A_W}, \tag{3.15}$$

where $q_{W,in}$ is the total flow rate of the water into the water continuous phase and the water dispersed into the oil phase and A_W is the area of the circular segment containing the water phase in which the oil droplets are being dispersed.

The area of the segment containing water A_W is given in (3.2).

The flowrate of liquid into the water continuous phase $q_{W,in}$ is the amount of water entering the water phase and the amount of dispersed oil entering the water phase

$$q_{W,in} = q_{L,in}\big(\alpha\phi_{ww} + \beta\phi_{ow}\big).$$

3.2.4 Vertical Velocity

The terminal velocity for the dispersed particles is given by *Stokes' Law*

$$v_v = \frac{g d_p^2(\rho_p - \rho)}{18\mu}, \tag{3.16}$$

where d_p is the diameter of the particle for every droplet class as mentioned in section 3.2.2, ρ_p is the density of the particle, ρ is the density of the continuous phase and μ is the viscosity of the continuous phase. The particles can be either water or oil droplets dispersed in their continuous phases.

Stokes' Law assumes that the particles are spherical in shape, the flow of the droplet is laminar and that the droplet movement is not hindered by the other droplets or the surface of the separator.

3.2.5 Horizontal and vertical residence time

In order to understand if the dispersed phase is being separated or is carried along with the bulk phase, it is important to understand the horizontal and the vertical residence times. The horizontal residence time for the droplets in their respective bulk phase can be defined as the amount of time the droplets spend in the separator before reaching their outlets.

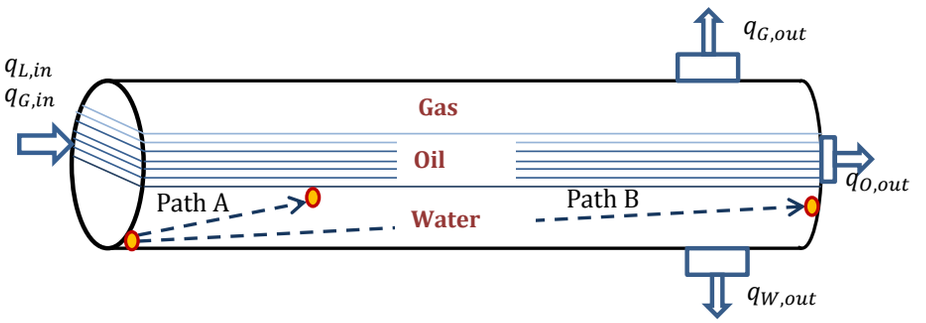

Figure 3.3: Illustration of the horizontal and the vertical residence times.

The horizontal residence time is given by the equation:

$$t_h = \frac{L}{v_h^{oil,water}}. \tag{3.17}$$

The dispersed particles are considered to be separated from the continuous phase, if they rise or fall vertically to reach the interface well within the time it takes for the dispersed phase to move horizontally along the length of the separator.

The vertical residence time is derived from the terminal velocity

$$t_v = \frac{h_{W,O}}{v_v}, \tag{3.18}$$

where $h_{W,O}$ is the height of water layer and the oil layer, and v_v is the vertical velocity of the droplets (see section 3.2.1 and 3.2.4).

Using these residence time comparisons, the number of droplets entering their respective homogeneous phases were calculated. Consequently, the total volume of the droplets leaving the bulk phase can be calculated.

It is understood that if the time taken by the droplets to reach the interface is less than the horizontal residence time, the droplets will reach their homogeneous phase before reaching the outlet. This is illustrated by the path A in Figure and if the time taken by the droplets to reach their outlet is lesser than the vertical residence time, the droplets will appear at their outlet and is illustrated by path B in Figure 3.3.

3.2.6 Separation Efficiency

In section 3.2.5, the time taken by the droplets to reach their homogeneous phase or remain in the continuous phase was described. Based on this, the number and volume of oil droplets entering into their homogeneous phase or dispersing in their continuous phase was estimated using a code scripted in MATLAB (see Appendix E.1) and similar calculations were made for the water droplets as well (see Appendix E.2).

Separation efficiency is an important factor in order to measure the performance of the pipe separator. Separation efficiency of oil is defined as the fraction of initially dispersed oil being removed from the water phase and is given by

$$\eta_O = 1 - \frac{\text{Volume of oil droplets contained in water outlet}}{\text{Initial volume of oil dispersed}}. \tag{3.19}$$

Similarly, separation efficiency of water is defined as the fraction of initially dispersed water being removed from the oil phase and is given by

$$\eta_W = 1 - \frac{\text{Volume of water droplets contained in the oil outlet}}{\text{Initial volume of water dispersed}}. \tag{3.20}$$

This means an efficiency value of 98% indicates that 2% of initially dispersed volume is contained at the outlet.

4 Controller Design

The three phase separation process is controlled to keep the operating point at their design value. The manipulated variables are $u = [q_{W,out}, q_{O,out}, q_{G,out}]$ and the controlled variables are $y = [h_W, h_L, p]$. The separation process is controlled by using three PI controller loops. The water height in the separator is maintained at its nominal value by manipulating the valve at the water outlet line of the separator. The liquid level is maintained at the desired value by manipulating the oil outlet and the water outlet valve and the system pressure is maintained at a constant value by adjusting the valve at the gas outlet line.

The oil and the water levels including the system pressure are maintained at their respective setpoints using the PI Controllers. The controllers were introduced in Simulink using the PID blocks contained in the Simulink library and by setting the D term to zero. The PI controllers were tuned using open loop simulations and the SIMC tuning rules (see Appendix D.1, D.2) to obtain the tuning parameters as discussed in section 2.3.2.

The inbuilt PI controller block uses the expression

$$C(s) = \left[P + \frac{I}{s}\right]. \tag{4.1}$$

By comparing the above expression to the transfer function in (2.8), the P and I terms can be obtained as

$$P = K_c,$$

$$I = \frac{K_c}{\tau_I},$$

where K_c and τ_I are the SIMC PI settings given by (2.12) and (2.13) respectively.

Table 4.1: Parameters for three PI controllers for gravity separator of length = 10 m and radius = 1.65 m.

	P	I
Water Level	- 6.16	- 0.31
Oil Level	- 5.86	- 0.29
System Pressure	- 0.36	-0.18

Table 4.2: Parameters for three PI controllers for pipe separator of length = 108.9 m and radius = 0.5 m.

	P	I
Water Level	-21	-1.05
Oil Level	-20	-1
System Pressure	-0.39	-0.19

5 Simulation

In this section, all the models (see section 3.2) implemented in MATLAB Simulink will be described. The results for the gravity separation and pipe separation systems are studied and interpreted in sections 5.2 and 5.3 respectively. The simulation parameters are taken from [1, 2] and included in Appendix A.

5.1 Implementation in MATLAB Simulink

Simulink is a programming environment developed by MathWorks for the purpose of simulation. There is a close integration between the Simulink and MATLAB environment.

Figure 5.1 represents the models drawn directly into Simulink using the subsystem block for each model. As the complexity of the model increased due to the total number of model equations and also the nonlinear term being involved in almost every equation, all the model equations were grouped as separate blocks into individual subsystems. The main advantage of using subsystem blocks in simulink model was to reduce the number of blocks that could be shown on the model window.

Since each subsystem in simulink has its input and the output ports connected to the other subsystems, the simulink interface was made as generic as possible by scripting a code in MATLAB. This code was scripted to programmatically simulate the model using *sim* function. This was done in order to make the models in simulink as generic as possible so that simulation parameters could be changed directly in MATLAB.

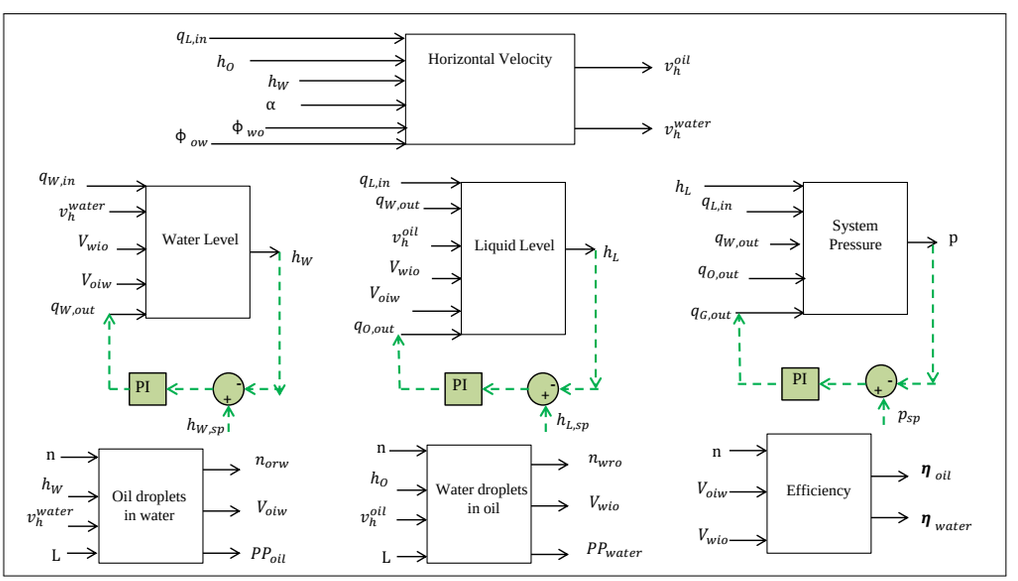

Figure 5.1: Schematic representation of the model introduced in MATLAB Simulink.

5.2 Horizontal Gravity Separator

The simulations for the three phase gravity separator is examined for two conditions.

- Simulations for initial production rates
- Simulation towards the end of the reservoir lifetime

5.2.1 Initial production rates

In this Section, the simulations are described based on the Gullfaks-A production rates. Gullfaks-A platform started its production during 1986-1987 [1, 2]. Table 5.1 presents the simulation parameters during the start-up of the well for a low water cut.

Table 5.1: Simulation parameters during the start-up of the well.

Parameter	Value
L	10 m
r	1.65 m
V_{Sep}	85.5 m^3
$q_{L,in}$	0.59 $m^3 s^{-1}$
α	0.135
β	0.865
ϕ_{wo}	0.3, 0.5, 0.7
ϕ_{wo}	0.3, 0.5, 0.7
p_{sp}	68.7 bar
$h_{W,sp}$	1.2 m
$h_{L,sp}$	2.5 m

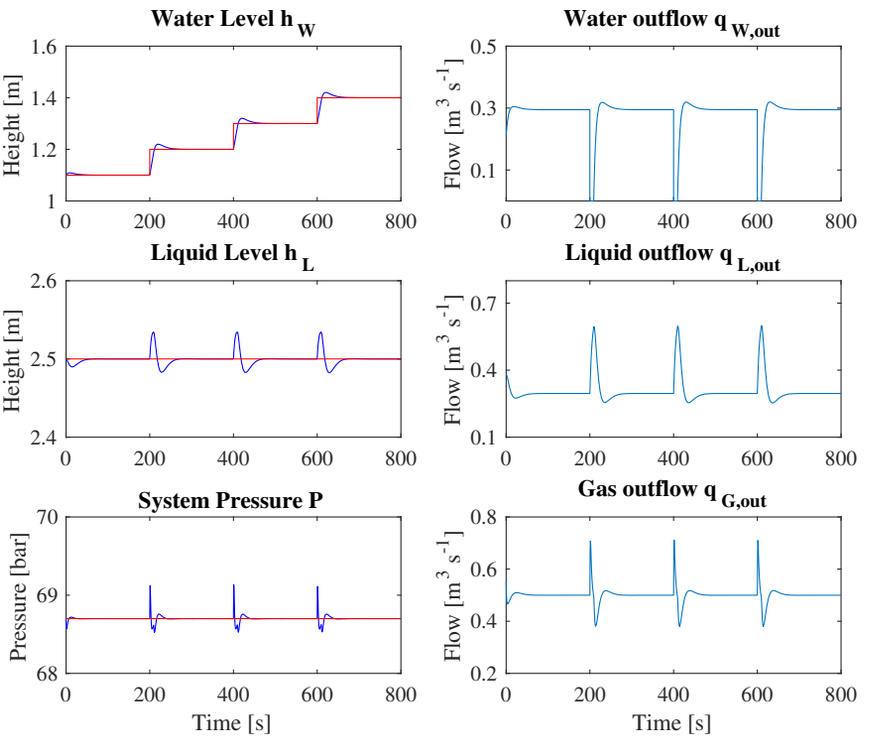

Figure 5.2: Controlled variables h_W, h_L and p with their respective manipulated variables $q_{W,out}$, $q_{O,out}$ and $q_{G,out}$.

In Figure 5.2, the plots on the left side show the variables to be controlled or in other words the state variables h_W, h_L and p. The three plots on the right side show their corresponding manipulated variables $q_{W,out}$, $q_{O,out}$ and $q_{G,out}$. It is observed from the Figure that the controlled variables are kept at their set-point values by the PI controllers where the set-point values are displayed in red.

As it is understood from the models described in section 3, the interface height has an influence on the horizontal velocity of the droplets and in turn influences the separation efficiency. Therefore, in order to analyze the overall separation efficiency of oil removal from the water phase and vice versa, the interface height was changed and hence the water height was varied in steps of +0.1 m for every 200 s, starting at an initial value of 1.1 m.

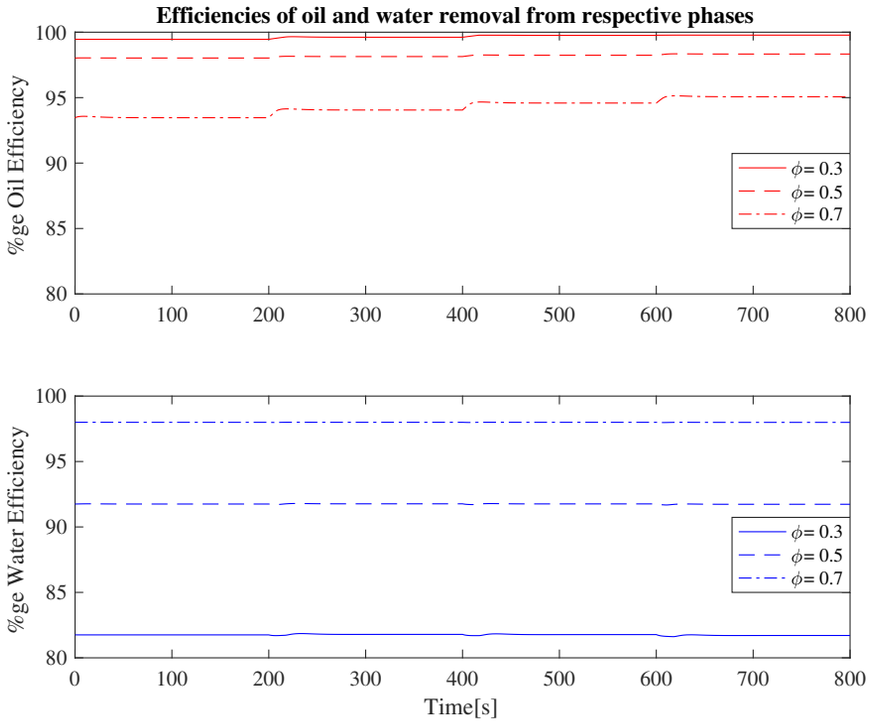

Figure 5.3: Efficiencies of oil (red) and water (blue) removal from their respective dispersed phase.

Based on the change in set-points of the water level as depicted in Figure 5.2, the efficiencies of oil removal from the water phase and the water removal from the oil phase are shown in Figure 5.3. Additionally, the separation efficiency was calculated for different initial separation values $\phi_{ow} = \phi_{wo} = 0.3$, $\phi_{ow} = \phi_{wo} = 0.5$ and $\phi_{ow} = \phi_{wo} = 0.7$.

It can be observed from the Figure that, as the initial amount of dispersed oil in the water phase ϕ increases, large amount of oil will appear at the water outlet, and hence the efficiency of the removal of oil from the water phase decreases. However, as the amount of water increases in the oil continuous phase, it can be observed that the efficiency of water removal from the oil phase increases. Therefore, it can be understood that the removal of dispersed oil from the continuous water phase is easier compared to the removal of dispersed water form the continuous oil phase.

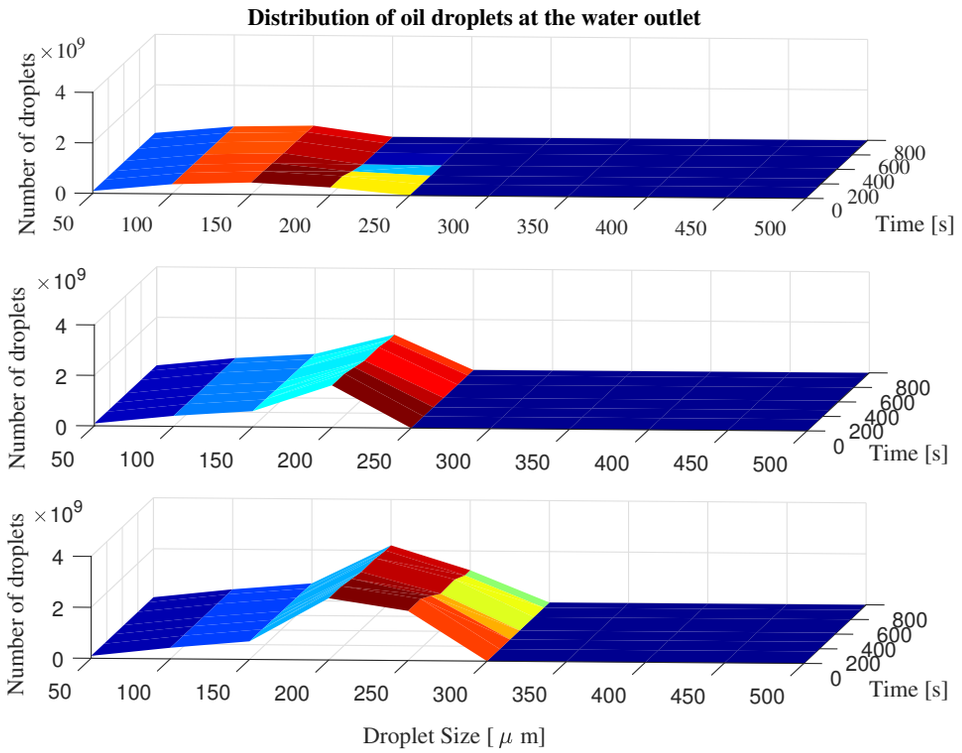

Figure 5.4: Number of oil droplets leaving at the water outlet for ϕ_{ow} = ϕ_{wo}= 0.3 (top) , ϕ_{ow} = ϕ_{wo} = 0.5 (center), ϕ_{ow} = ϕ_{wo} = 0.7 (bottom)

In Figure 5.4, the amount of oil droplets leaving the water outlet for the corresponding droplet size and time are shown for different values of the initial separation factor. At the top, the amount of oil droplets leaving the water phase is shown for ϕ_{ow} = ϕ_{ow} = 0.3. The plot at the center depicts the amount of oil leaving the water phase for ϕ_{ow} = ϕ_{ow} = 0.5 and the plot at the bottom shows the amount of oil droplets present at the water outlet for ϕ_{ow} = ϕ_{ow} = 0.7. The dark blue color in these plots indicate that all the oil droplets are being removed from the water phase.

It can be observed that with the increase in initial amount of oil entering the continuous water phase, the amount of oil droplets at the water outlet of the separator increases. The cut-off droplet size (minimum size above which the dispersed droplets present at the outlet is zero) of 250 μm is observed in case of ϕ_{ow} = ϕ_{ow} = 0.3 and 0.5, and 300μm for ϕ_{ow} = ϕ_{ow} = 0.7.

As the water height was increased by making step change of +0.1m every 200 s, the amount of oil droplets leaving the separator reduced.

5.2.2 Final production rates

This section describes the simulation for higher water cut and liquid flow rate for the same set-points and set-point changes as that of the initial production rates Table 5.2 shows the simulation parameters for the future production condition of the well.

Table 5.2: Simulation parameters for the end of the reservoir lifetime.

Parameter	Value
L	10 m
r	1.65 m
V_{Sep}	85.5 m^3
$q_{L,in}$	0.73 $m^3 s^{-1}$
α	0.475
β	0.525
ϕ_{wo}	0.3, 0.5, 0.7
ϕ_{wo}	0.3, 0.5, 0.7
p_{sp}	68.7 bar
$h_{W,sp}$	1.2 m
$h_{L,sp}$	2.5 m

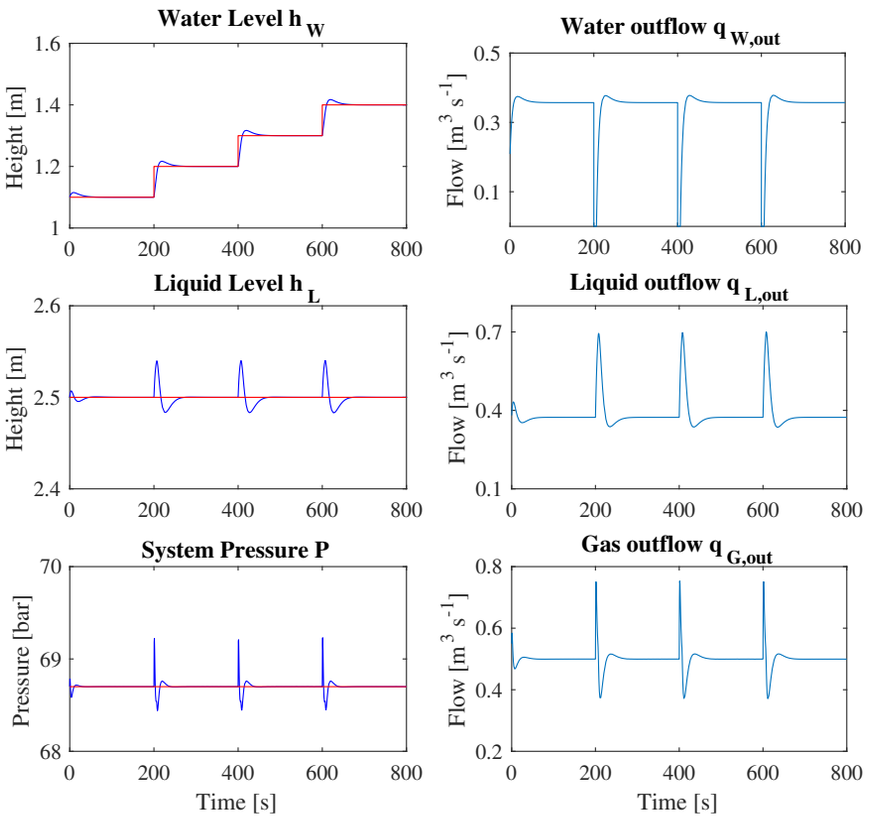

Figure 5.5: Controlled variables h_W, h_L and p with their respective manipulated variables $q_{W,out}$, $q_{O,out}$ and $q_{G,out}$.

In Figure 5.5, the plots on the left side show the variables to be controlled or in other words the state variables h_W, h_L and p. The three plots on the right side show the corresponding manipulated variables $q_{W,out}$, $q_{O,out}$ and $q_{G,out}$. It is observed from the Figure that the PI controllers keep the controlled variables at their set-point values by adjusting the manipulated variables. However, as a result of the increased value of water-cut α = 0.475 compared to the initial production, where α = 0.135, the outflows are different. The water level was varied in steps of +0.1m for every 200 s, starting at an initial value of 1.1 m.

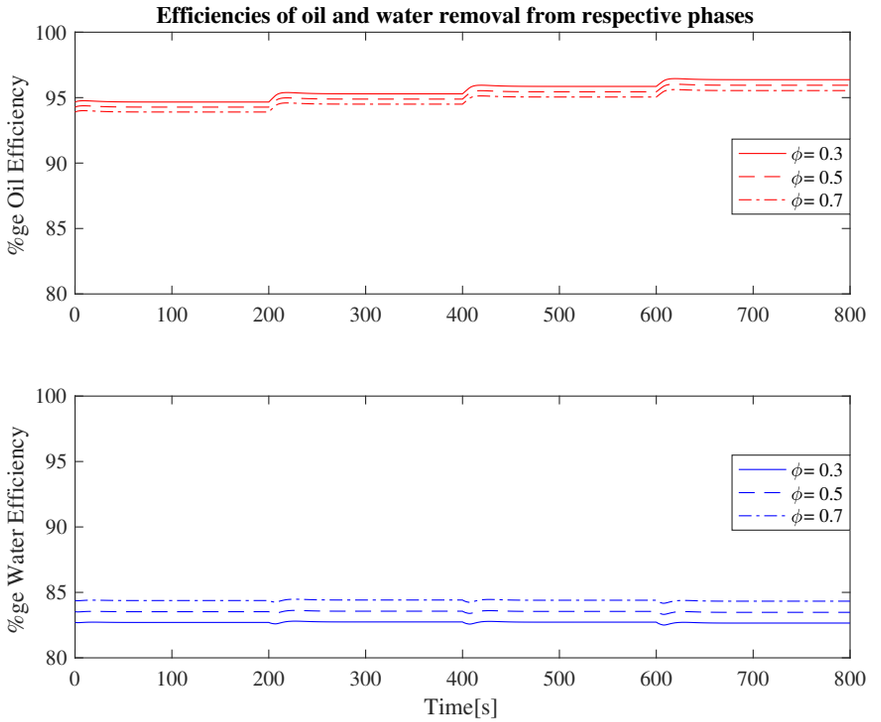

Figure 5.6: Efficiencies of oil (red) and water (blue) removal from their respective dispersed phase.

Figure 5.6 depicts the separation efficiencies for removal of oil droplets from the water phase and the removal of water droplets from the oil phase. The separation efficiency was compared for different initial separation values ϕ_{ow}= ϕ_{wo} = 0.3, 0.5 and 0.7.

It can be observed from the Figure that with the increase in water cut α, the separation efficiency of removal of oil droplets from the water phase is poor (for α = 0.135 and ϕ_{ow} = ϕ_{wo}= 0.3, the separation efficiency of oil is observed to be around 98%, and for the increased α = 0.475, for the same ϕ value, the separation efficiency is around 95%). In addition to this, as the amount of dispersed oil in the water phase increases, the efficiency of the removal of oil from the water phase decreases. Nonetheless, as the water level set-point increases, the removal of oil increases further.

From the Figure, it can be seen that the removal of water from the oil phase is almost uniform for increase in initial separation factors ϕ_{ow} and ϕ_{wo} and also for the change in set-point of the water level. Moreover, it can be observed that the increase in the initial separation values ϕ_{wo} and ϕ_{ow} do not influence the separation efficiency in this simulation case.

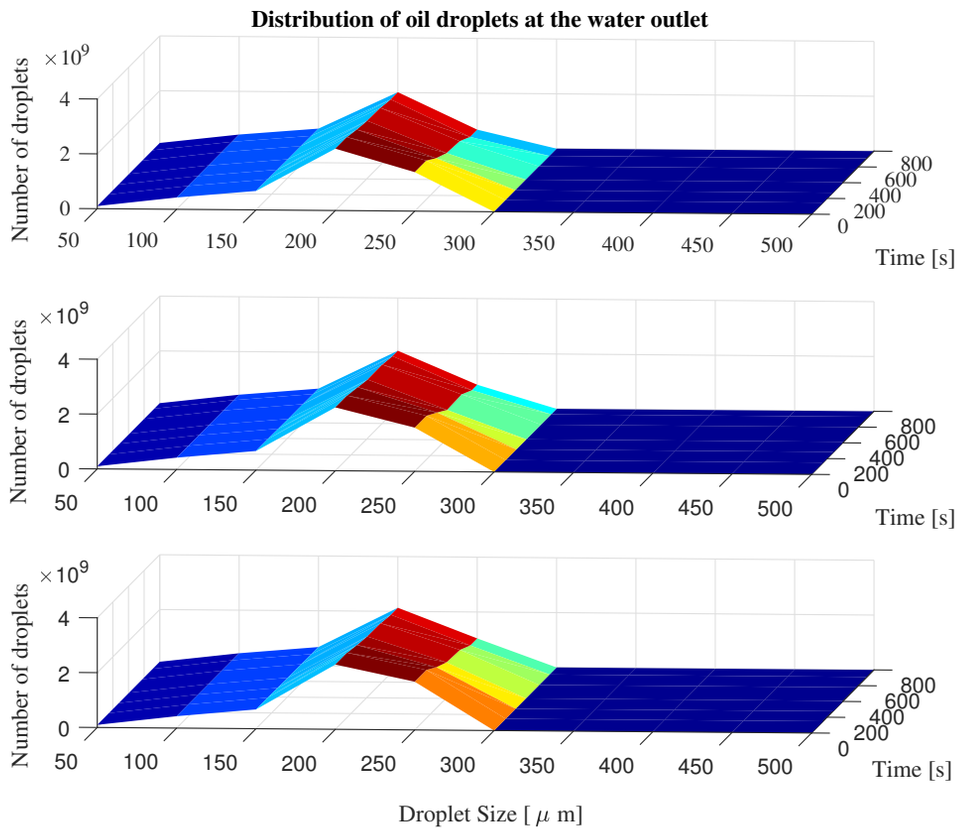

Figure 5.7: Number of oil droplets leaving at the water outlet for ϕ_{ow} = ϕ_{wo}= 0.3 (top) , ϕ_{ow} = ϕ_{wo} = 0.5 (center), ϕ_{ow} = ϕ_{wo} = 0.7 (bottom).

Figure 5.7 depicts the amount of oil droplets contained in the water outlet for the corresponding droplet size and time and also for the different initial separation values of ϕ_{ow} and ϕ_{wo}. The top plot shows the amount of oil droplets leaving the water phase for ϕ_{ow} = ϕ_{wo} = 0.3, the plot in the center shows the amount of oil droplets contained in the water phase for ϕ_{ow} = ϕ_{wo} = 0.5 and the bottom plot shows the number of droplets leaving at the water outlet for ϕ_{ow} = ϕ_{wo} = 0.7. The dark blue color in these plots indicate that all the oil droplets are being removed from the water phase.

It can be seen that all the three plots look alike since there is very small increase in the amount of oil droplets leaving the water phase as the initial separation values ϕ_{ow} and ϕ_{wo} increase unlike in Figure 5.4 where there is a significant increase in the oil droplets at the water outlet. The cut-off oil droplet size is at 300 μm for all the three plots and as the water level is increased in step size of +0.1m every 200 s, the oil droplets at the water outlet is reduced.

5.3 Horizontal Pipe Separator

This section describes the simulation results for a three phase horizontal pipe separator. Since the aspect ratio for the pipe separator is much higher than for the gravity separator, the length and the radius of the pipe separator were varied for a constant volume corresponding to that of the gravity separator.

Table 5.3 refers to the simulation parameters for the pipe separator.

Table 5.3: Simulation parameters for the horizontal pipe separator.

Parameter	Value
L	108.9 m
r	0.5 m
V_{Sep}	85.5 m^3
$q_{L,in}$	0.59 $m^3 s^{-1}$
α	0.135
β	0.865
ϕ_{wo}	0.3, 0.5, 0.7
ϕ_{wo}	0.3, 0.5, 0.7
p_{sp}	68.7 bar
$h_{W,sp}$	0.375 m
$h_{L,sp}$	0.75 m

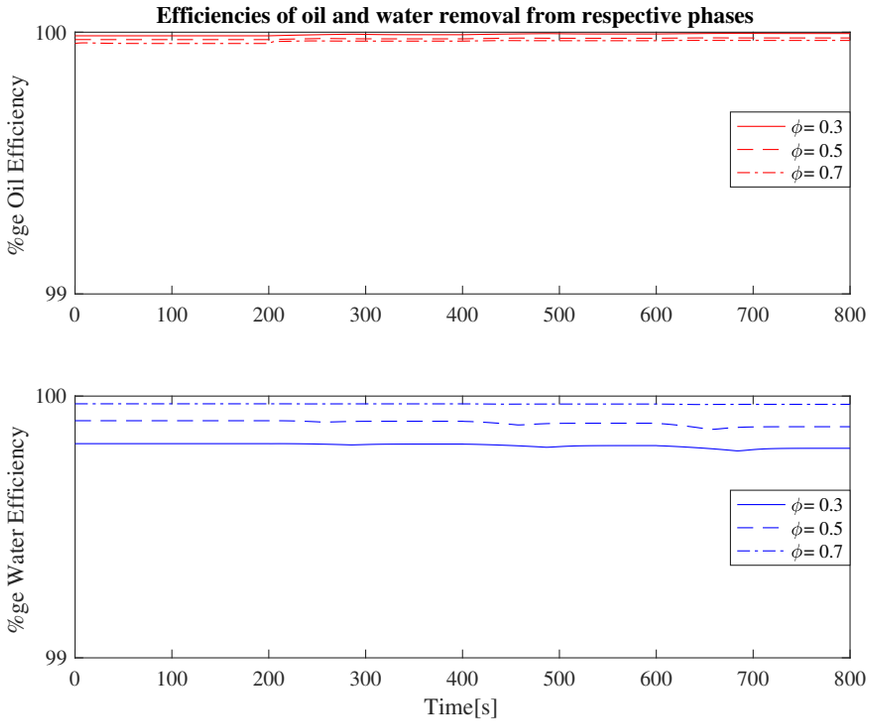

Figure 5.8: Efficiencies of oil (red) and water (blue) removal from their respective dispersed phase.

Figure 5.8 shows the separation efficiencies for removal of oil droplets from the water phase for different initial separation values ϕ_{ow} = ϕ_{wo} = 0.3, 0.5 and 0.7. In addition to this, water level was varied in step size of +0.05m for every 200 s, starting at an initial value of 0.37 m.

It is observed that for a pipe separator having a shorter radius and a much longer length, the efficiency of removal of oil from water phase as well as the efficiency of removal of water from the oil phase is very high for the same water cut α, in comparison to the separation efficiency of the gravity separator as illustrated in Figure 5.3.

It can be observed from the Figure, that the separation efficiencies for the removal of oil from the water and vice versa, is almost uniform both for the case of increased initial separation values ϕ_{ow} and ϕ_{wo}, and also for the step increase in the water level.

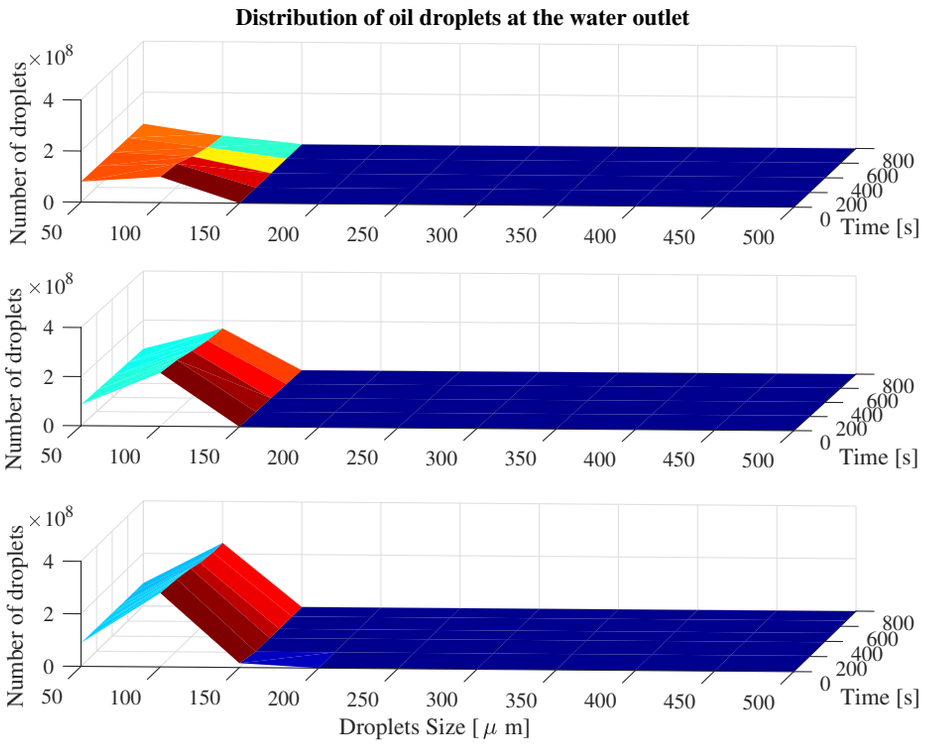

Figure 5.9: Number of oil droplets leaving at the water outlet for ϕ_{ow} = ϕ_{wo}= 0.3 (top) , ϕ_{ow} = ϕ_{wo} = 0.5 (center) , ϕ_{ow} = ϕ_{wo} = 0.7 (bottom).

Figure 5.9 illustrates the number of oil droplets leaving the water outlet of the pipe separator for the respective droplet size, time and for the different initial separation values ϕ_{ow} and ϕ_{wo}. The plots at the top, center and the bottom show the amount of oil droplets contained in the water phase for initial separation values of ϕ_{ow} = ϕ_{wo} = 0.3, 0.5 and 0.7, respectively.

It is observed that with an increase in initial separation values ϕ_{ow} and ϕ_{wo} the number of droplets remaining at the water outlet is insignificant in comparison with that of the gravity separator. As the water level is increased in step of +0.05m for every 200 s, the oil droplets leaving the water outlet is negligible. Additionally, the cut-off droplet size of 150 μm is observed for all the three plots which is much lesser when compared to the gravity separator in Figure 5.4, where the cut-off droplet size was 250 μm. All droplets above the size of 150 μm are separated since the pipe separator has a smaller radius and a longer length.

5.3.1 Pipe Separator: Effect of change in radius

From the previous sections on simulation of gravity and pipe separators, it was observed that for a smaller diameter and a longer length of the pipe separator, the separation efficiency for removal of oil droplets from the water phase and for the removal of water droplets from the oil phase was high. Consequently, the number of oil droplets at the water outlet was observed to be fewer in contrast to the gravity separator. Therefore, in this section the volume of oil droplets at the water outlet is calculated for a pipe separator for a constant length to investigate the effect of varying diameter on the separation efficiency.

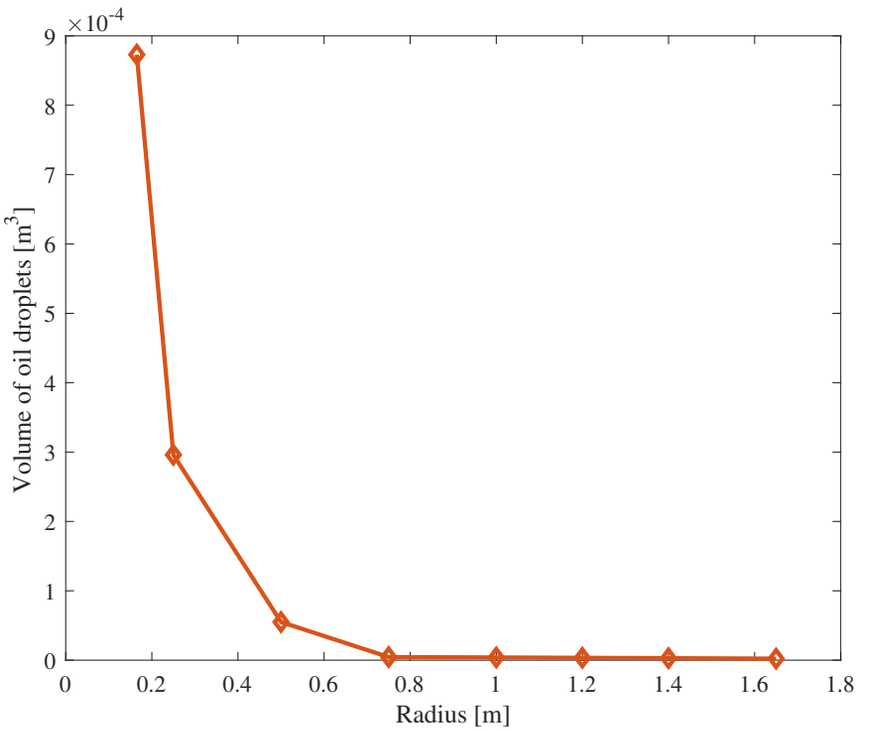

Figure 5.10: Volume of oil droplets at the water outlet for the pipe separator Length = 108.9 m.

In Figure 5.10, the volume of oil droplets remaining at the water outlet for the pipe separator with different radius is illustrated where radius $r \in \{0.165, 0.25, 0.5, 0.75, 1, 1.2, 1.4, 1.65\}$ and the remaining parameters are constant as shown in the table. It can be observed that there is an exponential decrease in the volume of oil contained at the water outlet as the diameter of the pipe increases. For a small pipe diameter, there is a substantial volume of oil present at the water outlet in contrast to the larger diameter pipe where only negligible amount of oil are present.

This nature of the plot is due to the fact that for a small diameter pipe, the horizontal velocity of the droplets is higher. Therefore the droplets take less time to reach the outlet in comparison to the time it takes to reach its interface. Hence the droplets move to the outlet before reaching their homogeneous phase.

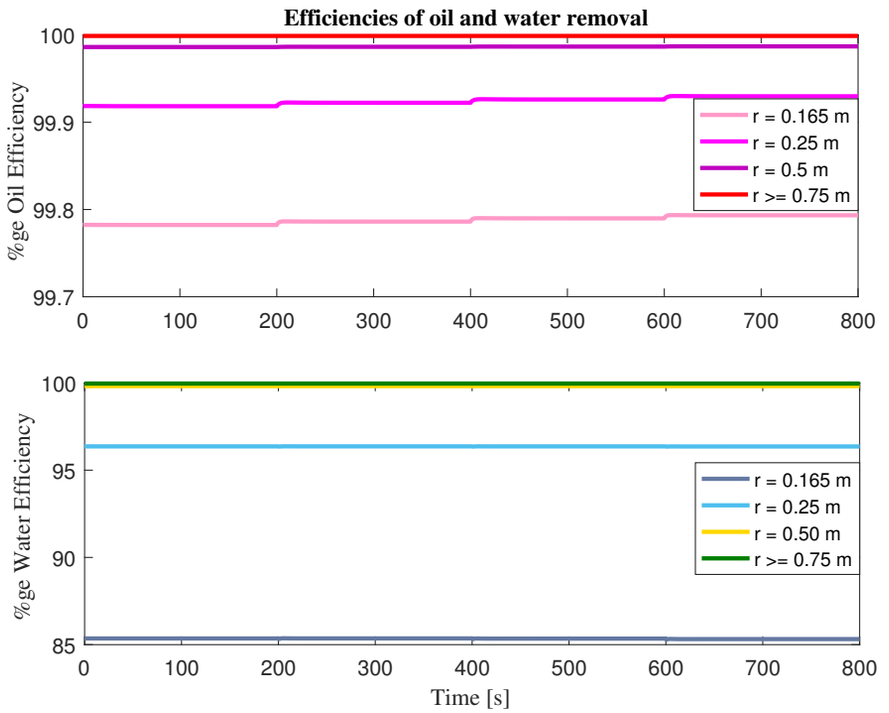

Figure 5.11: Efficiencies of oil (top) and water (bottom) removal for the pipe separator of Length = 108.9 m.

In Figure 5.11, the top plot illustrates the separation efficiency for the removal of oil droplets from the water phase and the bottom plot illustrates the separation efficiency for the removal of water droplets from the oil phase for a pipe separator of constant length and varying radii $r \in \{0.165, 0.25, 0.5, 0.75, 1, 1.2, 1.4, 1.65\}$. It is observed that as the radius of the pipe separator increases, the efficiency of removal of oil and water droplets increases.

5.3.2 Parallel pipe Separators

Case I: Effect of change in length

In section 5.3.1, a single pipe separator was studied for a range of diameters to observe the effect of pipe diameter on the separation efficiency. In this section, parallel pipe separators are studied to investigate their effect on the volume of oil droplets at the water outlet for all the pipes combined.

In Figure 5.10, it can be seen that for the radius of pipe separator larger than 0.75m, the volume of oil droplets at the water outlet is almost constant and negligible. Hence, *Case I* considers the minimum radius for which the volume of droplets is the least in Figure 5.10.

Table 5.4: Flow and the number of droplets entering each parallel pipe separator.

$q_{L,in}$ = 0.59 $m^3 s^{-1}$				
	A	B	C	D
Number of pipe separators in parallel	One	Two	Three	Four
Flow into each pipe separator	$q_{L,in}$	$\frac{1}{2}q_{L,in}$	$\frac{1}{3}q_{L,in}$	$\frac{1}{4}q_{L,in}$
Number of droplets entering each separator	n	$\frac{1}{2}n$	$\frac{1}{3}n$	$\frac{1}{4}n$

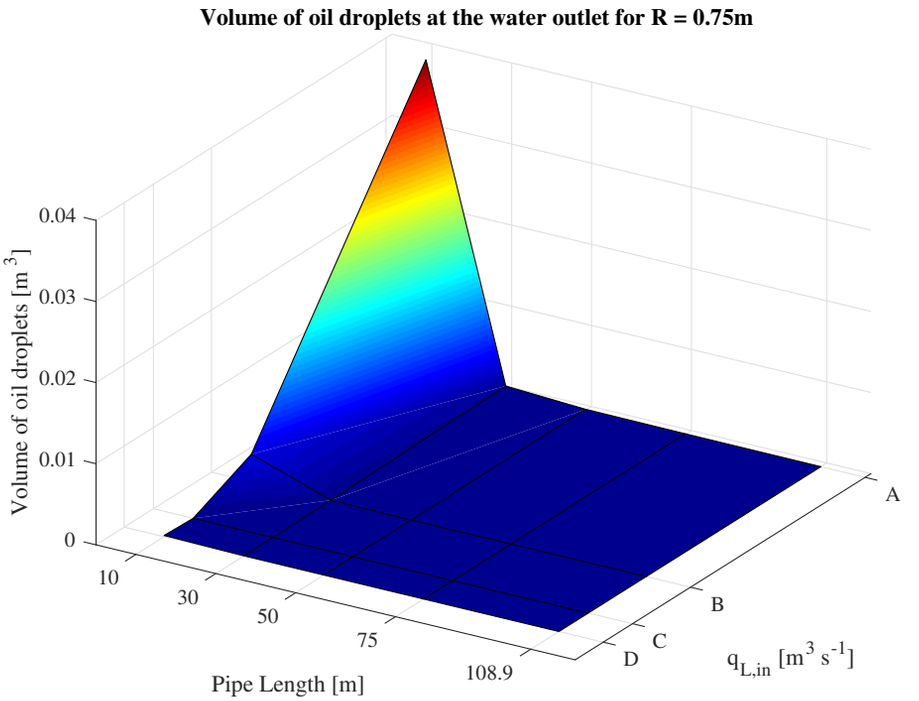

Figure 5.12: Combined total volume of oil droplets at the water outlet over all the parallel pipes each with radius = 0.75 m.

Figure 5.12 displays the volume of oil droplets at the water outlet over their respective pipe lengths and the flow rates into each parallel pipe separator having a radius of 0.75m. As seen, point A corresponds to a single pipe, and points B, C and D corresponds to two, three and four pipe separators placed in a parallel arrangement respectively. Table 5.4 refers to the liquid flow rate and the droplet distribution into each parallel pipe separator.

From the Figure, it can be observed that for a single pipe separator having a length of 10m, the volume of oil droplets at the water outlet is large and as the length of the pipe increases, the volume of oil at the water outlet decreases. In addition to this, the volume of oil decreases by utilizing several pipe separators in parallel.

In this case for a single pipe 30m long, the volume of oil droplets at the water outlet was same as that for three pipes each 10m long placed parallel to each other. Similarly, for two parallel pipes each 75m long, the volume of oil droplets at the water outlet was found to be the same as having three parallel pipes each 50m long (see Appendix C).

Case II: Effect of change in radius

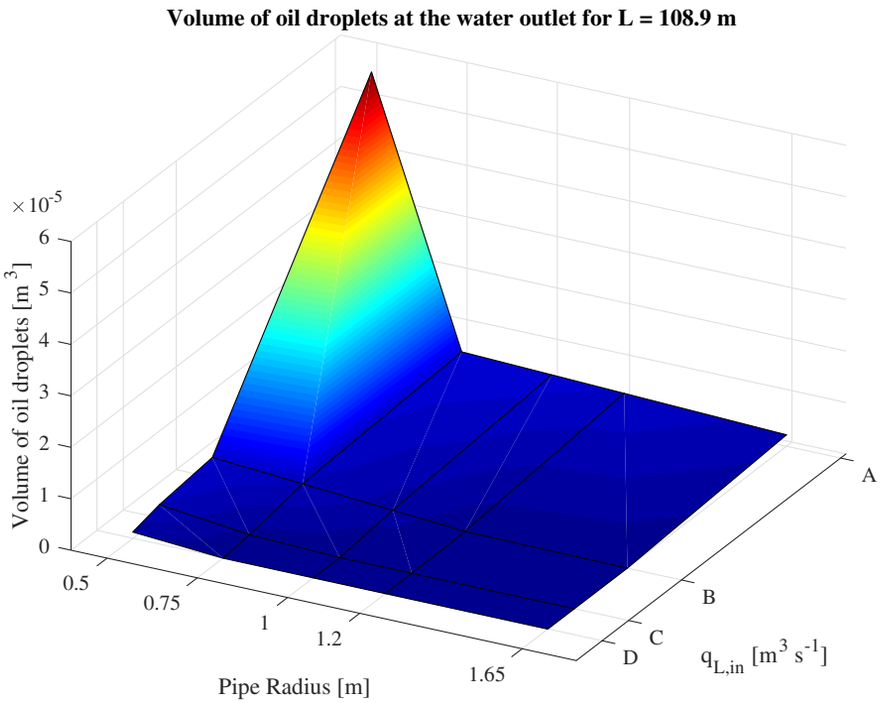

Figure 5.13: Volume of oil droplets at the water outlet for the pipe separator Length = 108.9 m.

Table 5.4 gives information about the liquid flow rate distributed into each parallel pipe separator and the number of droplets entering the separator. The droplets entering each parallel pipe separator are assumed to be equally distributed. In total, four cases have been considered as indicated by A, B, C, D in Figure 5.13. Point A corresponds to a single pipe separator whereas points B, C, D correspond to two, three and four pipe separators placed parallel to each other respectively . In addition, all the separators are studied for a constant length of 108.9 m.

From the Figure, it is observed that for a single pipe separator with a radius of 0.5m, the volume of oil droplets at the water outlet is relatively higher compared to the volume for an increase in radius of the pipe separator. As the number of parallel pipe separators increases, it can be observed that the volume of oil decreases at the common outlet of all the parallel separators.

In this case, it was seen that for two parallel pipes each with radius of 1m, the volume of oil droplets at the water outlet was observed to be same as that for four parallel pipes each with a radius of 0.5m . A similar observation was made for two parallel pipes each with a radius of 0.75m, the volume of oil at

the water outlet was observed to be same as that for three parallel pipes each with a radius of 0.5m (see Appendix B).

6 Conclusion

A three phase gravity and pipe separation system has been analysed in this report and model parameters have been taken from [1, 2]. The objective of the gravity separator study was to analyse the effect of different heights of water levels and the degree of initial separation at the inlet on the overall separation efficiency. The simulation results indicate that larger water levels are favourable for the quality of the water at the outlet of the separator. However, there was not much effect on the quality of oil outlet stream; in fact a decrease in oil quality with increase in water level was observed. It was also seen that with smaller initial separation factors (ϕ_{ow} and ϕ_{wo}), meaning for better pre-separation of oil and water phases, better overall separation efficiencies were noticed for both oil and water phases.

The simulation was conducted for a small diameter pipe separator having the same volume as the gravity separator. It was observed that the volume of oil droplets at the water outlet was much smaller in comparison to the gravity separator since the droplet traveling distance to the liquid interface is much shorter.

Since the pipe separator gave better efficiency in comparison to the gravity separator in terms of droplet removal from their respective phases, the simulation was carried out for pipe separators but various diameters. In this case it was seen that there was an exponential decrease in the volume of oil droplets at the water outlet. This is because even though the vertical residence time for the droplets is shorter in case of pipe separators, due to the reduced diameter of the pipe, the horizontal velocity of the droplets is much higher. This allows for a very short horizontal residence time in comparison to the vertical residence time.

Finally, the performance of parallel pipe separators was evaluated for two cases: constant length pipe separators of varying diameters and constant diameter pipe of varying lengths. In both cases, the volume of oil at the water outlet for all the pipe separators combined was estimated. It was noticed that with the increase in number of pipes placed in a parallel arrangement, the total volume of oil droplets at the water outlet was reduced. However, it could be observed that for a fixed pipe length, placing many equal diameter pipe separators in parallel was equivalent to a single large diameter pipe in terms of volume of oil droplets at the common water outlet. Similar observations were made for constant diameter parallel pipe separators, where placing several equal length pipe separators in parallel was equivalent to single pipe separator of longer length in terms of volume of oil droplets at the water outlet for all the pipes combined. The parallel configuration of pipe separators gives flexibility of operation in a real time setting rather than using a single large separator because the same system can be used throughout the lifetime of the reservoir in various configurations. Also having separators in parallel enables to operate at different processing capacities.

6.1 Future work

The fluid dynamics inside the separators involve a lot of complexity, and hence it is necessary to study the phenomena like droplet breakage and coalescence. In actuality, there exists an initial distribution of droplet size at the inlet of the separator, and the size distribution changes inside the separator due to non-uniform flow patterns and factors such as coalescence and droplet breakage. This evolution of the droplet size distribution can be estimated by the use of Population Balance Equations (PBE) and incorporating these models can further improve the exactness of estimation [16].

For the absence of droplet breakage and coalescence, only Stokes' law is sufficient to determine the terminal settling velocity of the droplets which has been considered for the purpose of modeling. However, while considering the coalescence and the break up of droplets which exists commonly in the separators, the velocity is hindered and the Stokes' law for settling will need to take into account the correction factor.

References

[1] C. J. Backi and S. Skogestad., "A simple dynamic gravity separator model for separation efficiency evaluation incorporating level and pressure control," Sept 2016, Preprint submitted to 2017 American Control Conference.

[2] A. P. Laleh, W. Y. Svrcek, and W. D. Monnery., "Computational fluid dynamics-based study of an oilfield separator–part II: An optimum design," *Society of Petroleum Engineers*, vol. 2, pp. 52 – 59, Feb 2013.

[3] C. Moraes, F. da Silva, and D. Oliveira., "Subsea versus topside processing - conventional and new technologies." http://dx.doi.org/10.4043/24519-MS: Offshore Technology Conference, Oct 2013.

[4] F. Albuquerque, O. Riberio, and M. Morais., "Subsea processing systems: Future vision." http://dx.doi.org/10.4043/24161-MS: Offshore Technology Conference, May 2013.

[5] S. Arnes, S. Abrand, and N. Butin., "New solutions for subsea produced water separation and treatment in deepwater." http://dx.doi.org/10.4043/22667-MS: Offshore Technology Conference, Oct 2011.

[6] S. Sagatun, P. Gramme, StatoilHydro, and F. Technologies., "The pipe separator: Simulations and experimental results." http://dx.doi.org/10.4043/19389-MS: Offshore Technology Conference, May 2008.

[7] A. Hannisdal and R. Westra., "Compact separation technologies and their applicability for subsea field development in deep water." http://dx.doi.org/10.4043/23223-MS: Offshore Technology Conference, May 2012.

[8] http://www.seabedseparation.no/.

[9] S. Wang and L. Gomez., "Compact multiphase inline water separation (iws) system - a new approach for produced water management and production enhancement." http://dx.doi.org/10.2118/104252-MS: Society of Petroleum Engineers, Dec 2006.

[10] C. Perez., "Horizontal pipe separator (HPS ©) experiments and modeling," Ph.D. dissertation, The University of Tulsa, http://tustp.org/publications/Ciro_Perez_Dissertation_2005.pdf, 2005.

[11] E. Pereyra., "A simplified mechanistic model for an oil/water horizontal pipe separator," Ph.D. dissertation, The University of Tulsa, http://dx.doi.org/10.2118/163077-PA, Jun 2013.

[12] S. LeBlanc and D. R. Coughanowr, *Process Systems Analysis and Control*, 3rd ed. McGraw Hill, 2009.

[13] D. E. S. et al., *Process Dynamics and Control*, 3rd ed. John Wiley & Sons, Jul 1993.

[14] S. Skogestad., "Simple analytic rules for model reduction and pid controller tuning," *Journal of Process Control*, vol. 13, pp. 291 – 301, Jun 2003.

[15] D. Rivera, M. Morari, and S. Skogestad., "Internal Model Control. 4. PID Controller Design," *Ind. Eng. Chem. Process Des. Dev*, pp. 252 – 265, Jan 1986.

[16] J. Slot, "Development of a centrifugal in-line separator for oil-water flows," Master's thesis, Universitet Twente, Jun 2013.

A Simulation Parameters

Table A.1: Simulation Parameters [1, 2].

Parameter	Description	Value
M_G	Molar mass of the gas	0.01604 $kg\,mol^{-1}$
R	Universal gas constant	8.314 $kg\,m^2\,s^{-2}\,mol^{-1}\,K^{-1}$
T	Temperature	328.5 K
g	Gravitational acceleration	9.8 $m\,s^{-2}$
$q_{G,in}$	Volumetric gas inflow	0.456 $m^3\,s^{-1}$
μ_O	Viscosity of oil	0.001 $kg\,(m\,s)^{-1}$
μ_W	Viscosity of water	0.0005 $kg\,(m\,s)^{-1}$
ρ_G	Density of gas	49.7 $kg\,m^{-3}$
ρ_O	Density of oil	831.5 $kg\,m^{-3}$
ρ_W	Density of water	1030 $kg\,m^{-3}$

B Volume of oil at water outlet for constant length parallel pipes: L = 108.9 m

Table B.1: Combined total volume of oil droplets at the water outlet over all the parallel pipes each with Length = 108.5 m

Length = 108.9 m, $q_{L,in}$ = 0.59 $m^3 s^{-1}$			
Radius	Volume of oil droplets at the water outlet	Flow into each separator	Number of separators
1.65	2.21e-6		
1.2	3.39e-6		
1	3.91e-6	$q_{L,in}$	One
0.75	4.56e-6		
0.5	55.2e-6		
1.65	0		
1.2	0.24e-6		
1	1.28e-6	$\frac{1}{2}q_{L,in}$	Two
0.75	2.59e-6		
0.5	3.91e-6		
1.65	0		
1.2	0		
1	0	$\frac{1}{3}q_{L,in}$	Three
0.75	0.61e-6		
0.5	2.6e-6		
1.65	0		
1.2	0		
1	0	$\frac{1}{4}q_{L,in}$	Four
0.75	0		
0.5	1.28e-6		

C Volume of oil at water outlet for constant radius parallel pipes: R = 0.75 m

Table C.1: Combined total volume of oil droplets at the water outlet over all the parallel pipes each with radius = 0.75 m

Radius = 0.75 m, $q_{L,in}$ = 0.59 $m^3 s^{-1}$			
Length	Volume of oil droplets at the water outlet	Flow into each separator	Number of separators
10	38500e-6	$q_{L,in}$	One
30	624e-6		
50	122e-6		
75	49.14e-6		
108.9	4.56e-6		
10	3400e-6	$\frac{1}{2}q_{L,in}$	Two
30	92e-6		
50	4.73e-6		
75	3.82e-6		
108.9	2.59e-6		
10	624e-6	$\frac{1}{3}q_{L,in}$	Three
30	5.29e-6		
50	3.82e-6		
75	2.46e-6		
108.9	0.61e-6		
10	154e-6	$\frac{1}{4}q_{L,in}$	Four
30	4.36e-6		
50	2.91e-6		
75	1.1e-6		
108.9	0		

D Controller tuning

Three PI controllers were employed to control the water level, total liquid level and the system pressure at their desired set-point values. In order to obtain the parameters for PI controller, tuning of the controllers was done using open-loop step response method to obtain the model information and the SIMC tuning rules. Section D.1 shows the calculations of the PI controller parameters for the gravity separator of length = 10m and radius = 1.65m and section D.2 shows the calculations for the pipe separator of length = 108.9m and radius = 0.5m.

D.1 Tuning of a gravity separator with open loop step responses

TUNING OF THE WATER LEVEL

In order to tune the water level in the gravity separator, a 10% step change was performed. The plot of open loop step response of the water level is shown in Figure D.1.

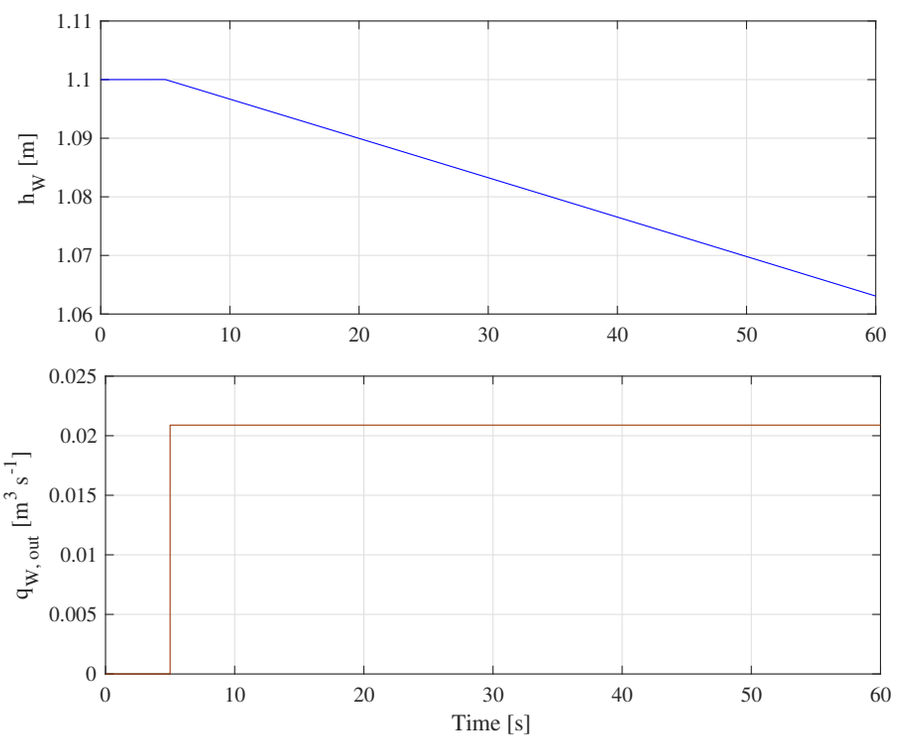

Figure D.1: Open loop response of the water level for a given setpoint change in manipulated variable $q_{W,out}$.

From the Figure, it can be seen that it is an integrating process with time delay of θ = 0 s. A desired closed loop time constant τ_c = 5 s is assumed. The FOPTD parameters are calculated as described in section 2.3.1.

$$k' = \frac{\Delta y}{\Delta u \Delta t} = \frac{(1.065 - 1.1)}{0.021(57 - 5)} = -0.0321$$

$$K_c = \frac{1}{k'(\tau_c + \theta)} = -6.15$$

$$\tau_I = 4(\tau_c + \theta) = 20$$

Therefore PI parameters are given by

$$P = K_c = -6.15$$

,

$$I = \frac{K_c}{\tau_I} = -0.31$$

.

TUNING OF THE TOTAL LIQUID LEVEL

In order to tune the total liquid level, a 10% step change was made in outlet oil flowrate $q_{O,out}$. The plot of open loop step response is shown in Figure D.2.

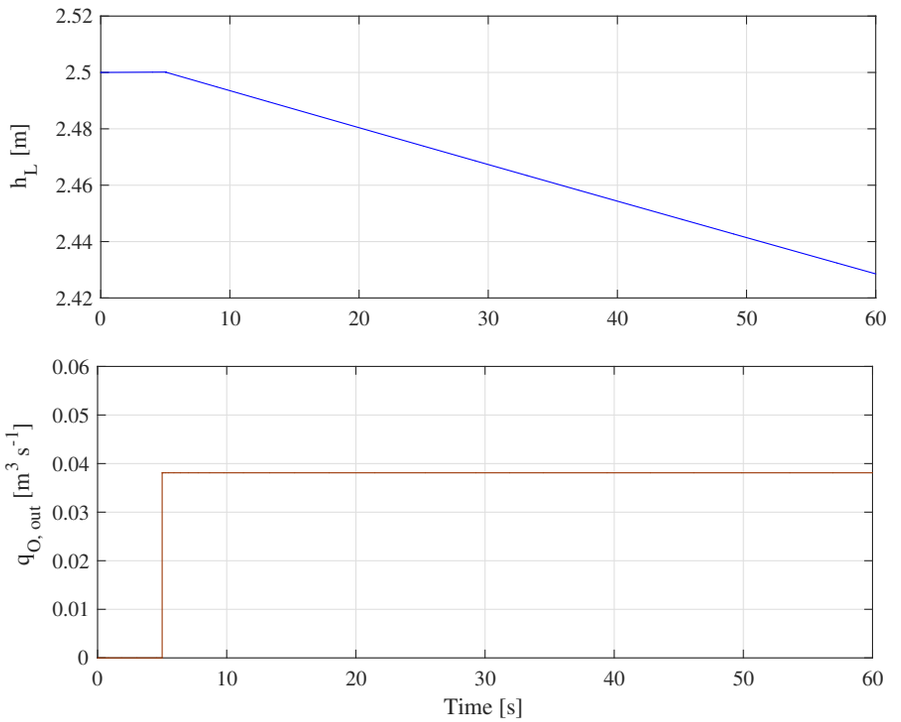

Figure D.2: Open loop response of the water level for a given setpoint change in manipulated variable $q_{O,out}$.

From the Figure, it can be noticed that it is an integrating process with time delay of θ = 0 s. A desired closed loop time constant τ_c = 5 s is assumed. The FOPTD parameters are calculated.

$$k' = \frac{\Delta y}{\Delta u \Delta t} = \frac{(2.432 - 2.5)}{0.038(57 - 5)} = -0.0344$$

$$K_c = \frac{1}{k'(\tau_c + \theta)} = -5.86$$

$$\tau_I = 4(\tau_c + \theta) = 20$$

Therefore PI parameters are given by

$$P = K_c = -5.86$$

;

$$I = \frac{K_c}{\tau_I} = -0.29$$

.

TUNING OF THE SYSTEM PRESSURE

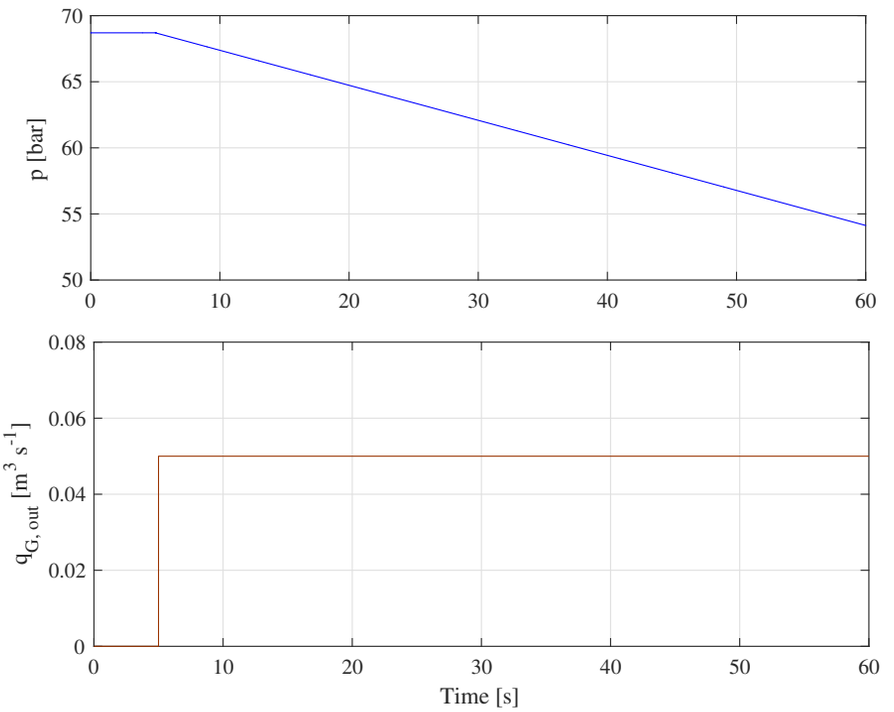

Figure D.3: Open loop response of the water level for a given setpoint change in manipulated variable $q_{W,out}$.

In order to tune the system pressure, a 10% step change was made in outlet gas flowrate $q_{G,out}$. The plot of open loop step response is shown in Figure D.3. A desired closed loop time constant τ_c = 5 s is assumed. The FOPTD parameters are calculated as follows.

$$k' = \frac{\Delta y}{\Delta u \Delta t} = \frac{(54.92 - 68.7)}{0.05(57 - 5)} = -5.32$$

$$K_c = \frac{1}{k'(\tau_c + \theta)} = -0.36$$

$$\tau_I = 4(\tau_c + \theta) = 2$$

Therefore PI parameters are given by

$$P = K_c = -0.36$$

,

$$I = \frac{K_c}{\tau_I} = -0.18$$

.

D.2 Tuning of a pipe separator with open loop step responses

TUNING OF THE WATER LEVEL

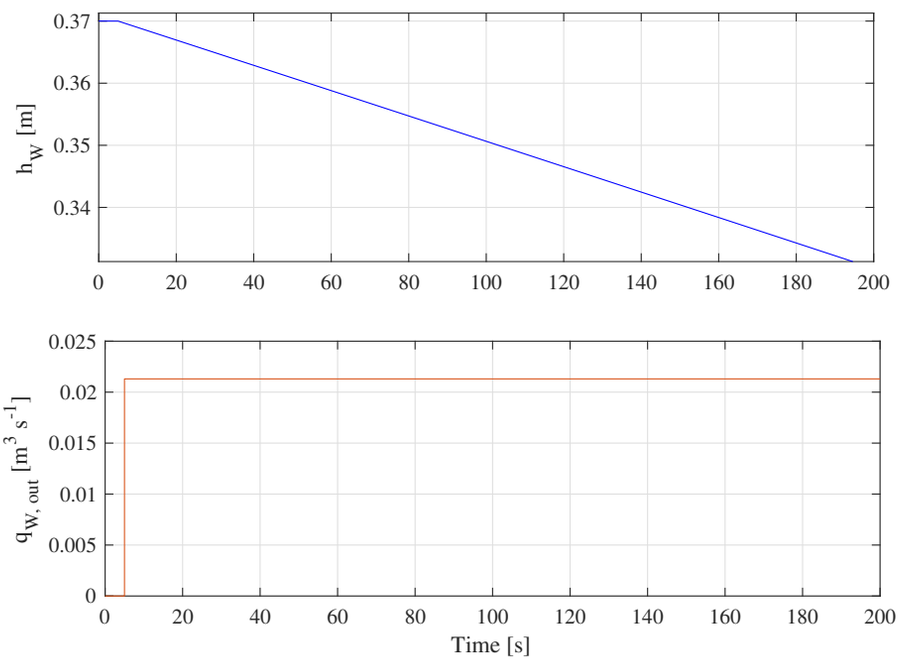

Figure D.4: Open loop response of the water level for a given setpoint change in manipulated variable $q_{W,out}$.

In order to tune the water level in the pipe separator, a 10% step change was performed on its manipulated variable $q_{W,out}$. The plot of open loop step response of the water level is shown in Figure D.4.

From the Figure, it can be seen that it is an integrating process with time delay of θ = 0 s. A desired

closed loop time constant τ_c = 5 s is assumed. The FOPTD parameters are calculated as described in section 2.3.1.

$$k' = \frac{\Delta y}{\Delta u \Delta t} = \frac{(0.331 - 0.37)}{0.0213(197 - 5)} = -0.0095$$

$$K_c = \frac{1}{k'(\tau_c + \theta)} = -21$$

$$\tau_I = 4(\tau_c + \theta) = 20$$

Therefore PI parameters are given by

$$P = K_c = -21$$

,

$$I = \frac{K_c}{\tau_I} = -1.05$$

.

TUNING OF THE TOTAL LIQUID LEVEL

In order to tune the total liquid level, a 10% step change was made in outlet oil flowrate $q_{O,out}$. The plot of open loop step response is shown in Figure D.5.

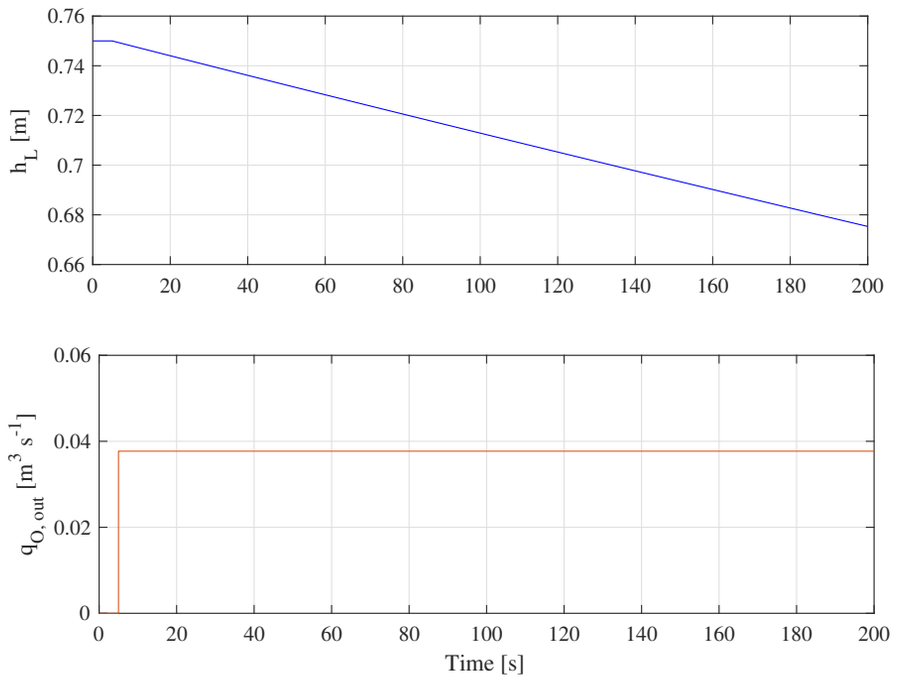

Figure D.5: Open loop response of the water level for a given setpoint change in manipulated variable $q_{O,out}$.

From the Figure, it can be noticed that it is an integrating process with time delay of θ = 0 s. A desired closed loop time constant τ_c = 5 s is assumed. The FOPTD parameters are calculated.

$$k' = \frac{\Delta y}{\Delta u \Delta t} = \frac{(0.68 - 0.75)}{0.038(197 - 5)} = -0.01$$

$$K_c = \frac{1}{k'(\tau_c + \theta)} = -20$$

$$\tau_I = 4(\tau_c + \theta) = 20$$

Therefore PI parameters are given by

$$P = K_c = -20$$

,

$$I = \frac{K_c}{\tau_I} = -1$$

.

TUNING OF THE SYSTEM PRESSURE

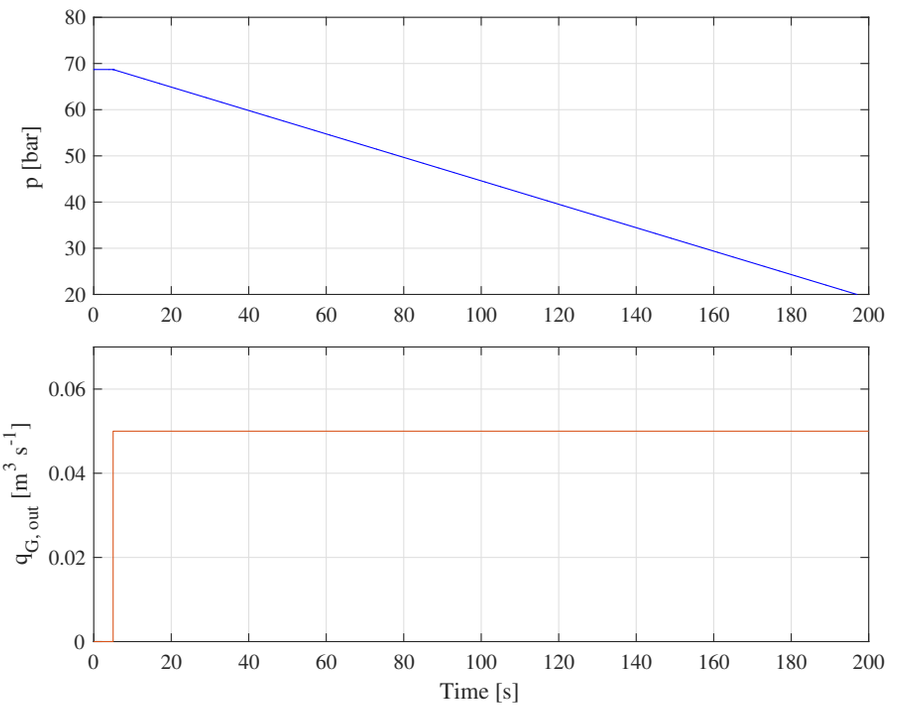

Figure D.6: Open loop response of the water level for a given setpoint change in manipulated variable $q_{W,out}$.

In order to tune the system pressure, a 10% step change was made in outlet gas flowrate $q_{G,out}$. The plot of open loop step response is shown in Figure D.6. A desired closed loop time constant τ_c = 5 s is assumed. The FOPTD parameters are calculated as follows.

$$k' = \frac{\Delta y}{\Delta u \Delta t} = \frac{(19.9 - 68.7)}{0.05(197 - 5)} = -5.08$$

$$K_c = \frac{1}{k'(\tau_c + \theta)} = -0.39$$

$$\tau_I = 4(\tau_c + \theta) = 2$$

Therefore PI parameters are given by

$$P = K_c = -0.36$$

,

$$I = \frac{K_c}{\tau_I} = -0.19$$

.

E MATLAB code

In order to estimate the amount of oil droplets present in the water phase and vice versa, a code is scripted in MATLAB based on the horizontal and the vertical residence times of the droplets and position of droplets in the separator. Section E.1 presents the code to estimate the amount of oil droplets contained in the water phase and section E.2 presents the water droplets contained in the oil phase.

E.1 Calculation of oil droplets contained in water continuous phase

```
function [noil_new, Voil_new, lpp_oil_new]  = oildroplets_in_water(
   v_horizontal, h_water, n, L)

% v_horizontal is the horizontal velocity of oil droplets.
% h_water is the height of the water.
% n is the vector of initial oil particles size distribution.
% L is the length of the pipe.
% d is the vector of diameter of all the oil particles.
% s is the vertical velocity of the droplets.
% V is the volume of oil droplets
d = zeros(1,10)';
V = zeros(1,10)';
s = zeros(1,10)';
lpp_oil_new = zeros(1,10)';
noil_new = zeros(1,10)';
Voil_new = zeros(1,10)';
density_oil = 831.5;
density_water = 1030;
dyn_visc_water = 0.5e-3;

for i = 1:10
    d(i) = 50*10^(-6)*i;
    V(i) = 4/3*pi*(d(i)/2)^3;
    s(i) = abs(((d(i))^2)*9.81*(density_oil-density_water)/(18*
       dyn_visc_water));

    if (L/v_horizontal)>= ( h_water/s(i))
```

```
26          noil_new(i) = 0; % number of oil droplets present in the
               water phase
27          Voil_new(i) = n(i)* V(i); % volume of oil droplets leaving
               the water phase
28          lpp_oil_new(i)= h_water; % position of the oil particles
29      else
30          lpp_oil_new(i)= (L/v_horizontal)*s(i);
31          noil_new(i) = (1-(lpp_oil_new(i)/h_water))* n(i);
32          Voil_new(i) = n(i) * V(i)*(lpp_oil_new(i)/h_water);
33      end
34  end
```

E.2 Calculation of water droplets in oil continuous phase

```
1   function [nwater_new, Vwater_new,lpp_water_new]  =
       waterdroplets_in_oil(v_horizontal, h_liquid, h_water, n, L)
2
3   % v_horizontal is the horizontal velocity of water droplets.
4   % h_water is the height of the water.
5   % n is the vector of initial water particles size distribution.
6   % L is the length of the pipe.
7   % d is the vector of diameter of all the water particles.
8   % s is the vertical velocity of the droplets.
9   % V is the volume of water droplets
10
11  h_oil = h_liquid - h_water;
12  d = zeros(1,10)';
13  V = zeros(1,10)';
14  s = zeros(1,10)';
15  lpp_water_new = zeros(1,10)';
16  nwater_new = zeros(1,10)';
17  Vwater_new = zeros(1,10)';
18  density_oil = 831.5;
19  density_water = 1030;
20  dyn_visc_oil =1e-3;
21
```

```
22 for i = 1:10
23     d(i) = 50*10^(-6)*i;
24     V(i) = 4/3*pi*(d(i)/2)^3;
25     s(i) = abs(((d(i))^2)*9.81*(density_oil-density_water)/(18*
           dyn_visc_oil));
26
27     if (L/v_horizontal)>= (h_oil/s(i))
28         nwater_new(i) = 0; % number of water droplets present in the
               oil phase
29         Vwater_new(i) = n(i)* V(i); % volume of water droplets
               leaving the oil phase
30         lpp_water_new(i)= h_water; % position of the water particles
31     else
32         lpp_water_new(i)= (L/v_horizontal)*s(i);
33         nwater_new(i) = (1-(lpp_water_new(i)/h_oil))* n(i);
34         Vwater_new(i) = n(i) * V(i)*(lpp_water_new(i)/h_oil);
35     end
36 end
```